Nanoscale Horizons

ROYAL SOCIETY OF CHEMISTRY

REVIEW

View Article Online
View Journal | View Issue

Cite this: *Nanoscale Horiz.*, 2023, **8**, 1313

Nanofibrous scaffolds for the healing of the fibrocartilaginous enthesis: advances and prospects

Xin Li,†[a] Yan Ren,†[ab] Yueguang Xue,[b] Yiming Zhang[b] and Ying Liu *[b]

With the current developmental advancements in nanotechnology, nanofibrous scaffolds are being widely used. The healing of fibrocartilaginous enthesis is a slow and complex process, and while existing treatments have a certain effect on promoting their healing, these are associated with some limitations. The nanofibrous scaffold has the advantages of easy preparation, wide source of raw materials, easy adjustment, easy modification, can mimic the natural structure and morphology of the fibrocartilaginous enthesis, and has good biocompatibility, which can compensate for existing treatments and be combined with them to promote the repair of fibrocartilaginous enthesis. The nanofibrous scaffold can promote the healing of fibrocartilaginous enthesis by controlling the morphology and ensuring controlled drug release. Hence, the use of nanofibrous scaffold with stimulative response features in the musculoskeletal system has led us to imagine its potential application in fibrocartilaginous enthesis. Therefore, the healing of fibrocartilaginous enthesis based on a nanofibrous scaffold may be a novel therapeutic approach.

Received 31st May 2023,
Accepted 11th August 2023

DOI: 10.1039/d3nh00212h

rsc.li/nanoscale-horizons

1. Introduction

The interface where tendons or ligaments attach to bones is called an enthesis, and its role is to smoothly transition the stress from soft tissue to hard tissue, promote joint movement, and transfer physiological loading.[1] Degeneration of enthesis can be caused by injury, disease, and aging.[2] The enthesis can be broadly classified as direct (fibrocartilaginous) or indirect attachment (fibrous) according to the structure.[3] Fibrous enthesis is the connection between tendons or ligaments and collagen fibers in bone through Sharpey fibers.[4] Fibrocartilaginous enthesis healing typically consists of four different regions: tendons/ligaments, non-mineralized fibrocartilage, mineralized fibrocartilage, and bone, including the insertion of rotator cuff, anterior cruciate ligament (ACL), Achilles tendon, and patellar tendon.[1,5] These are also the most common clinical locations for injury and are the main focus of this study. Damage to the fibrocartilaginous enthesis can lead to

[a] *School of Public Health, Zhejiang Chinese Medical University, Hangzhou, 310053, China*
[b] *CAS Key Laboratory for Biomedical Effects of Nanomaterials and Nanosafety & CAS Center for Excellence in Nanoscience, National Center for Nanoscience and Technology of China, Beijing, 100190, China. E-mail: liuy@nanoctr.cn; Tel: +86 1082545526*
† These authors contributed equally to this work.

Xin Li

Xin Li is a master's degree candidate at the School of Public Health at Zhejiang Chinese Medicine University, Hangzhou, China. Her current research focuses on tissue repair.

Yan Ren

Yan Ren obtained her bachelor's degree (2021) from Southern Medical University, China. She is currently a postgraduate researcher in the National Center for Nanoscience and Technology of China and Zhejiang Chinese Medical University. Her research interests are focused tissue repair.

severe disability and likely, osteoarthritis.[3] At present, the main treatment methods for rotator cuff and ACL are surgical repair and reconstruction.[6] Although the repair and reconstruction techniques for ligaments/tendons continue to improve, they still have limitations.[7] For example, in ACL reconstruction surgery, autologous transplantation has drawbacks such as relatively long tendon bone interface healing time, expensive surgery, and poor long-term efficacy.[10,89] It is estimated that there are over 100 000 cases of ACL reconstruction in the United States alone each year, with a cost of over $1.5 billion.[11] As the gold standard for treating rotator cuff tears, the incidence of retearing can even reach 94%.[12,13] Surgical repair and reconstruction typically only restore the anatomical structure of the fibrocartilaginous enthesis, and the scar tissue formed after healing lacks natural gradient structure and collagen fiber arrangement, resulting in poor mechanical properties that do not promote fibrocartilaginous enthesis regeneration.[14,15] In addition, some non-surgical therapies also have limitations. As is known, the natural healing process of the injury is complex, including inflammation, rapid proliferation, and gradual remodeling.[14] Although musculoskeletal tissue has natural self-healing ability, its efficiency is relatively low.[16] Therefore, improving the healing of fibrocartilaginous enthesis poses great challenges.[1]

At present, various materials are widely used in the field of biomedicine.[17–27] Nanofibrous scaffolds made of various materials have shown their potential in nanotechnology.[28] Nanofibers are fibers with a diameter ranging from 1 to 1000 nm.[29] The small diameter of the nanofibers is very consistent with the extracellular matrix (ECM).[29] Nanofibrous scaffolds is an artificial ECM that can mimic the natural tissue environment. Its large surface area-to-volume ratio can effectively promote cell adhesion, proliferation, differentiation, and drug loading.[29,30] In recent years, nanofibrous scaffolds have been widely used in the field of tissue engineering.[31–36] The morphology of nanofibrous scaffolds is easy to adjust, as it appears that simulating the composition and structure of fibrocartilaginous enthesis is more beneficial to its regeneration and improving the mechanical properties of tissues. Nanofibrous scaffolds can control drug release during early healing of fibrocartilaginous enthesis. This is reflected not only in the continuous release of a very low concentration throughout the body but also in the significant reduction of side effects of the drug. In addition, electrospun nanofibers have been endowed with ''stimulus response'' properties to enable a variety of new applications.

The review focuses on the application of nanofibrous scaffolds in fibrocartilaginous enthesis healing. Some existing therapies to promote healing of fibrocartilaginous enthesis will also be briefly described. Nanofibrous scaffolds as a type of nanotechnology show their unique characteristics such as controllable morphology, controlled release of drugs, and stimulus response characteristics, which have been explored in this review. In summary, nanofibrous scaffolds have great potential for application in the field of promoting fibrocartilaginous enthesis healing.[37–41]

2. Healing mechanism of fibrocartilaginous enthesis injury

Fibrocartilaginous enthesis is a layered organization with multiple scales, which is beneficial for minimizing force

Yueguang Xue

Yueguang Xue is a PhD student at South China University of Technology, China. His research interest is the application of biomimetic functional materials in tissue repair.

Yiming Zhang

Yiming Zhang is a master at the Henan Institute of Advanced Technology, Zhengzhou University. She completed her master's degree in Physical Chemistry in 2023 at Zhengzhou University in conjunction with the National Center for Nanoscience and Technology. Her research interests include the fundamentals and applications of electrostatic spinning technology in tendon tissue engineering, and the use of multiple types of materials as tissue engineering scaffolds.

Ying Liu

Ying Liu received her bachelor's degree in 2000 from Tianjin Medical University and a PhD degree in 2006 from the Academy of Military Medical Sciences. In 2015, she was promoted to Professor in National Center for Nanoscience and Technology. She has published 140 research papers, including Nat Commun, Acc Chem Res, Nano Lett, PNAS, etc. She has won National Natural Science Outstanding Youth Foundation. Her research interests are mainly focused on tissue repair.

concentration to the greatest extent possible.[42,43] Each region exhibits unique characteristics in terms of cell type, ECM, collagen arrangement, and mineralization, which helps to effectively transmit stress and promote mutual fixation of bone and soft tissue grafts.[5,14,44] The main component of ECM in tendon/ligament area is type I collagen (Col I) (about 60–85% of its dry weight), and the rest is composed of proteoglycan, glycosaminoglycan (GAG), glycoprotein, and other collagen subtypes.[45] Non-mineralized fibrocartilage is rich in type II collagen, with high levels of type III collagen, and a small amount of type I and X collagen, decorin, and polysaccharides. Mineralized fibrocartilage is composed of hypertrophic fibrochondrocytes, ECM is mainly composed of type II collagen and a large amount of type X collagen and aggrecan.[5] The boundary between these two fibrocartilage regions is delineated by a "tidal marker", which represents the boundary between soft and hard tissues.[46] Finally, mineralized fibrocartilage is fused into the bone tissue area containing osteoblasts, osteocytes, and osteoclasts, as well as Col I and hydroxyapatite.[5,8] When a sudden load is applied in the direction of muscle stress, the tensile performance of the tendon end is better than that of the bone end.[30]

The natural healing process of the fibrocartilaginous enthesis is complex and can be divided into three stages: inflammation (0–7 days), rapid proliferation (5–14 days), and gradual remodeling (>14 days).[8] Fibrocartilaginous enthesis healing is typically usually achieved by the formation of disorganized fibrovascular scar tissue rather than natural gradient tissue regeneration. Abnormal or inadequate genetic expression, insufficient undifferentiated cells at the healing interface, and excessive mechanical load on the healing tendon can lead to the formation of disorganized fibrovascular scar.[47]

In the early stage of fibrocartilaginous enthesis injury, the levels of inflammatory factors such as interleukin (IL)-1β, IL-6, IL-8, tumor necrosis factor (TNF), matrix metalloproteinase (MMP)-1, MMP-3, and MMP-13 have been reported to be up-regulated.[14] At the same time, the release of chemokines (including vascular endothelial growth factor (VEGF), transforming growth factor beta (TGF-β), and platelet-derived growth factor (PDGF)) at the fibrocartilaginous enthesis recruits fibroblasts, which in turn recruit neutrophils, macrophages, and osteoclasts to the injury site to repair the damaged tendons, ligaments, fibrocartilage, and bone.[48] However, excessive production of reactive oxygen species (ROS) by immune cells during the inflammatory stage can cause fibrosis at the enthesis, leading to the formation of excessive scar tissue and poor biomechanical properties.[37,49] Because scar tissue with low biomechanical properties lacks a gradient structure and collagen fiber arrangement similar to natural fibrocartilaginous enthesis, this results in an increased risk of re-injury.[50] Even after surgical repair, the incidence of re-tearing after repair surgery can be as high as 94%.[12] Therefore, early inhibition of inflammation is essential to promote fibrocartilaginous enthesis healing.

During the rapid proliferative phase, fibroblasts, fibroblasts, fibrochondrocytes, osteocytes, and vascular endothelial cells proliferate rapidly, and fibroblasts produce collagen type III (the major component of scar tissue).[14,51] It has been suggested that TGF-β1 reaches peak levels at this stage and is abundant in fibrous scar tissue.[52] This may be a therapeutic target to prevent scar tissue formation.

During the final remodeling phase, the total cell density decreased and the production of collagen and GAG decreased, and the production of Col I increased progressively. Moreover, the number of fibroblasts continued to increase and the deposited collagen III was converted into highly organized collagen I.[14,53] In the rat rotator cuff insertion site model, it was found that although the structural properties of the healing

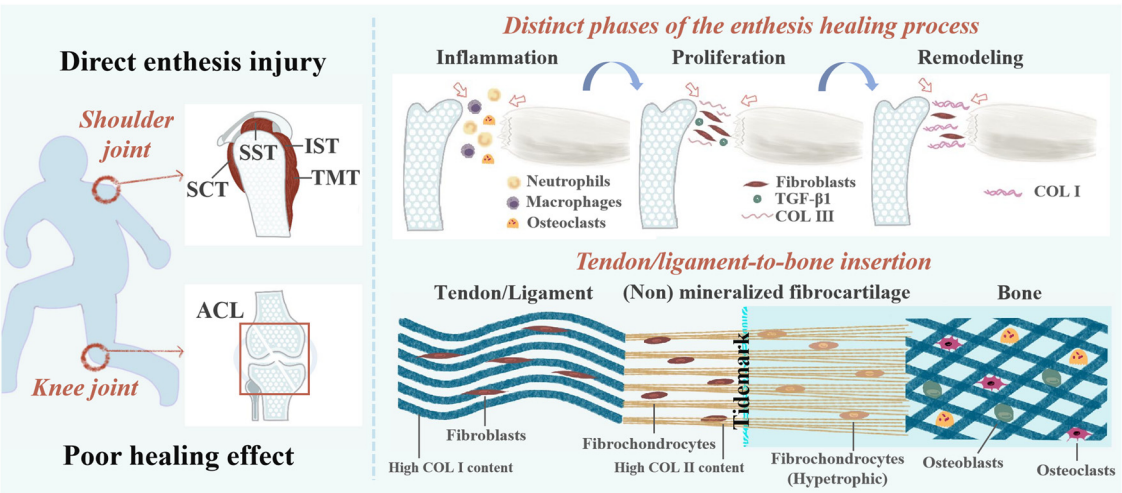

Fig. 1 The structure of the fibrocartilaginous enthesis and the healing mechanism. Injury to the fibrocartilaginous enthesis occurs most frequently in the shoulder and knee joints, and the healing process goes through inflammatory, proliferative, and remodeling phases. The structure of the fibrocartilaginous enthesis consists of tendons/ligaments, non-mineralized fibrocartilage, mineralized fibrocartilage, and bone. Abbreviations: SST, supraspinatus tendon; IST, infraspinatus tendon; SCT, subscapularis tendon; TMT, teres minor tendon; TGF-β, transforming growth factor beta; Col I, type I collagen; Col II, type II collagen.

tissue reached two-thirds of the undamaged specimen after 8 weeks, it was still significantly weaker.[46] Complete regeneration of the fibrocartilaginous enthesis has not been achieved.[54] The structure and healing mechanism of the fibrocartilaginous enthesis is shown in Fig. 1.

3. Existing therapies at the healing of the fibrocartilaginous enthesis

3.1 Limitations of existing therapies

Currently, a number of therapies are available to promote healing of the fibrocartilaginous enthesis (Fig. 2). Rotator cuff repair (RCR) and ACL reconstruction surgery remain the primary treatments for injuries or tears at the fibrocartilaginous enthesis, although the choice of surgical therapy is influenced by a variety of factors, such as patient's age, symptoms, and desired effect.[55,56] For example, to protect the meniscus and articular cartilage, the guidelines of the American Academy of Orthopaedic Surgeons (AAOS) highlights that ACL reconstruction surgery should be performed.[57] However, autologous transplantation as the main clinical method in ACL reconstruction surgery has drawbacks such as relatively long healing time, high costs, and poor long-term efficacy. Furthermore, they even carry a risk of infection.[8,9,10] Nonetheless, compared with physical therapy and unhealed rotator cuff repairs, moderate evidence supports that healed rotator cuff repairs show improved patient-reported and functional outcomes.[58] Furthermore, an observation of functional, radiological, and revision rates at least 10 years after RCR showed that the total recurrence rate of rotator cuff tears in asymptomatic patients can reach 30%.[59]

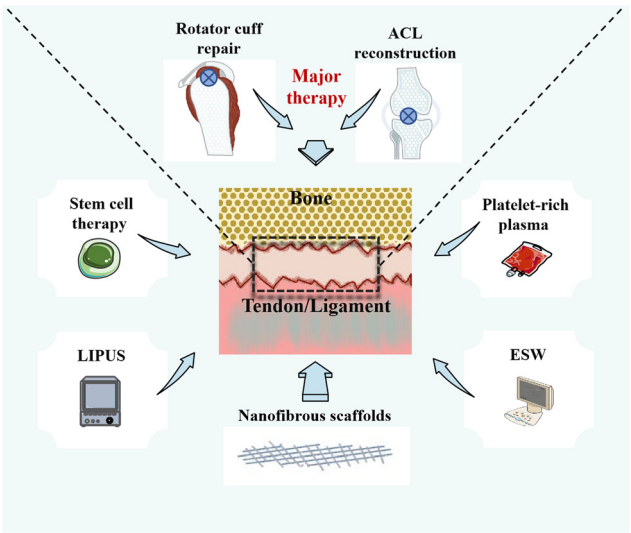

Fig. 2 Existing therapies to promote healing of fibrocartilaginous enthesis. The main therapeutic approaches to promote fibrocartilaginous enthesis healing include surgical repair and reconstruction, followed by stem cell therapy, platelet-rich plasma, LIPUS, ESW, and nanofibrous scaffolds to assist surgical repair. Abbreviations: ACL, anterior cruciate ligament; LIPUS, low-intensity pulsed ultrasound; ESW, extracorporeal shock wave.

In addition to surgical repair and reconstruction, researchers have been developing adjunctive treatments based on the physiological process of fibrocartilaginous enthesis healing for the past decade, such as stem cell therapy,[60] platelet-rich plasma (PRP),[61] and local physiotherapy.[62] First, the main objective of using stem cell therapy is to improve the healing environment of the fibrocartilaginous enthesis and simulate enthesis healing process by differentiating mesenchymal stem cells (MSCs) into different tissues.[63,64] However, there is a high risk of cell death when using stem cell therapy, thereby making it difficult to adhere to the tissue in need of repair.[12] In addition, although some studies have injected stem cells into the site of injury, the same site cannot be ensured for each injection. Therefore, it is difficult to guarantee its reliability.[64]

Second, PRP therapy is performed by centrifuging autologous blood to obtain platelets that can be applied locally to damaged tissues to improve healing.[65] Studies have shown that the use of PRP during tendon implantation into bone tunnel can induce fibrocartilage formation to promote fibrocartilaginous enthesis healing and relieve pain.[61,66] However, because of individual differences, the concentration and platelet activity of autologous PRP are difficult to control.[67] Furthermore, the American Academy of Orthopaedic Surgeons (AAAS) clinical practice guidelines state that there is no high level of evidence to support the use of platelet-derived products for biologically enhanced RCR, and that the evidence for the reduction of RCR with PRP is limited.[58] Third, physical therapy with non-invasive characteristics has been gradually applied to promote fibrocartilaginous enthesis healing.[68,69] Low-intensity pulsed ultrasound (LIPUS) has been shown to improve the healing of fibrocartilaginous enthesis by increasing the osteogenic differentiation of mesenchymal stem cells to promote the remodeling of fibrocartilaginous enthesis.[70] Unfortunately, its impact on the enthesis is mainly observed on the bone.[71] In addition, extracorporeal shock wave (ESW) therapy can promote the regeneration of bone and fibrocartilage at the fibrocartilaginous enthesis, and play a positive role in delaying the healing.[72] However, ESW has potential adverse effects, such as skin pain and redness, accounting for 4.8% and 21.1%, respectively.[69] Hence, physical therapy has potential side effects and treatment-site limitations.

Strategies such as growth factors, exosomes, and even gene therapy have also been applied to promote fibrocartilaginous enthesis healing.[73–75] However, these therapies also have the limitation of having to be combined with biomaterials to control their release, the relatively small number of studies that make their application difficult in clinical practice, and the need to confirm their biosafety.[7,54] In short, these therapies can improve the healing of the fibrocartilaginous enthesis in some ways, but there are still limitations that need to be addressed.

3.2 Nanotechnology at the healing of the fibrocartilaginous enthesis

Nanotechnology has been widely used in the field of prevention, diagnosis, and treatment of diseases.[76–79] In the field of

medical imaging, nanotechnology can overcome the limitations of nuclear medicine reagents in molecular imaging and improve the possibility of low-radiation, high-resolution imaging of diseases.[28] Compared with traditional drug therapy, nanotechnology can regulate the distribution and targeted accumulation of drugs and reduce drug toxicity.[80] In the field of regenerative medicine, nanoparticles have a larger surface area to promote cell adhesion than traditional scaffolds, and have good biocompatibility and stimulus response. However, nanoparticles do not have a continuous structure like nanofibers; thus, nanofibers are more suitable as scaffolds than nanoparticles.[28]

Over the past two decades, nanofibers have found widespread use in various biomedical fields. Human tissues and organs are composed of nanofibers in the ECM, and nanofibers can mimic the layered structure of the ECM, which facilitates cell adhesion and nutrient transport.[31,81] By changing the structure and properties of nanofibers such as porosity, diameter, alignment, patterning, surface functional groups, and mechanical properties, cell differentiation and controlled release of drugs can be promoted, to enhance the skin, nerve, blood vessels, and musculoskeletal system and tissue interface repair. In addition, electrospun nanofibers with ''stimulus-responsive'' properties such as shape memory, self-cleaning, self-healing, and sensing have been widely developed.[82] Nanofibrous scaffolds have high surface area-to-volume ratio, easy adjustment, and easy modification, which make them very attractive for repair at the fibrocartilaginous enthesis.[32,38,83]

Various methods such as electrospinning, phase separation, molecular self-assembly, use of bacterial cellulose (BC), template synthesis technique, and drawing process can be used to prepare nanofibrous scaffolds in the field of tissue engineering.[84–86] Nanofibrous scaffolds used for fibrocartilaginous enthesis repair are mainly prepared by electrospinning, self-assembly, and phase separation. Among them, electrospinning technology is the most widely used.[34] Compared with the others, electrospinning technology has the advantages of low-cost, high operability, versatility, and flexibility.[87] In the process of electrospinning, the polymer solution forms a polymer jet after electrostatic charge, mechanical pumping, and gravity. The increase in surface charge density during flight causes the ejected jet to extend and form nanofibers.[88] Nanofibers manufactured by electrospinning technology have more porous structures and a larger surface-to-volume ratio than those manufactured by other techniques; this also creates better conditions for cell attachment and the loading and delivery of drugs or other bioactive molecules, and has great application potential in the field of tissue repair.[36,89] In phase separation technology, the polymer is dissolved in the solvent and quickly cooled with the poor polymer of the induced solution and the rich polymer. Then, the solvent is exchanged with water and the material is frozen and dry, and the proper gelling temperature leads to nanofiber formation.[36] Similar to electrospinning technology, phase separation technology also has the characteristics of easy and simple manufacturing, but its processing time is long, and it is difficult to control the structure and stability of nanofibers. More importantly, the polymer used in phase separation technology has certain limitations and is not as abundant as the polymer that can be used in electrospinning.[36,90,91] A powerful approach for fabricating novel supramolecular architectures is molecular self-assembly.[92]

In self-assembly technology, noncovalent interactions between molecules are usually activated by factors such as temperature, acid–base level (pH) to build nanofibers from proteins, small molecules, peptides, and nucleic acids.[36] The nanofibers made by self-assembly are thinner than those made by electrospinning and are on the small end of the natural ECM scale.[92,93] However, the use of self-assembly technology to manufacture nanofibers has obvious disadvantages, such as complex processing, low productivity, high cost, and poor mechanical properties of the manufactured nanofibers, which may limit their application in tissue engineering.[36,94]

Nanofibrous scaffolds can be prepared using a variety of materials with different properties, enabling the preparation to meet the different requirements of tissue repair. The materials most commonly used for nanofibrous scaffolds are polymers, which can be classified as natural or synthetic polymers according to their source.[30,95] Natural polymers include fibroin, gelatin, collagen, and chitosan, which have excellent biocompatibility and biodegradability in common, and are conducive to cell proliferation, adhesion, and differentiation.[34] However, natural polymers have poor mechanical properties and often need to be used with synthetic polymers.[96] The synthetic polymers are polylactic acid (PLA), polyglycolic acid (PGA), and poly(lactic-*co*-glycolic acid) (PLGA) and polycaprolactone (PCL), which have the advantages of easy processing, can change size according to needs, and slow degradation.[34] However, as synthetic polymers degrade in the body, acidic products build up, occasionally leading to an inflammatory response. The hydrophobicity of some synthetic polymers even leads to reduced cell-scaffold interaction.[34] Therefore, to make nanofibrous scaffolds better suited to the needs of tissue repair, researchers have blended natural and synthetic polymers to produce nanofibrous scaffolds that combine the advantages of both. To make nanofibrous scaffolds work better, natural synthetic polymers can be mixed. The hybrid nanofiber scaffold not only has the biocompatibility and biodegradability of natural polymers, but also has excellent mechanical properties.[74] A summary of the synthetic methods, fundamental properties, materials, and advantages and disadvantages of the nanofibrous scaffolds for fibrocartilaginous enthesis repair is presented in Table 1.

4. Nanofibrous scaffolds for the healing of fibrocartilaginous enthesis

Currently, many therapies have been used clinically to promote fibrocartilaginous enthesis healing, including surgical reconstruction and other non-surgical therapies such as stem cell therapy, chemical and biological agents, and biophysical modalities.[54] Although these can improve the healing of the

Table 1 A summary of the synthetic methods, fundamentals, characteristics, ingredients and their advantages and disadvantages of nanofibrous scaffolds for fibrocartilaginous enthesis repair

Synthetic method	Fundamentals	Characteristics	Ingredients	Advantages	Drawbacks
Electrospinning	The uniaxial stretching of a viscoelastic solution[145]	Simple efficient low-cost controllability extensive materials	SF[37,74,116]	Biocompatibility Biodegradability ECM-like[34,146,147]	Slow degradation Poor cell recruitment performance Poor mechanical properties
			CS[118]	Biocompatibility Biodegradability High hardness	Poor mechanical properties
			Gelatin[38]	Low-cost, Biodegradability	Fast decomposition Low mechanical strength
			Col I[148]	Biocompatibility Biodegradability Biological activity Promote adhesion, proliferation, and differentiation[34]	Poor mechanical properties
			PLLA[108,149–151]	Biodegradability Biocompatibility Tractability	Slow degradation
			Poly(ester urethane) urea (PEUU)[152,153]	Biocompatibility Biodegradability Flexibility Easy processing[154]	Unfavorable for cell proliferation
			Polyurethane (PU)[96]	Good mechanical strength Biocompatibility Easy to process[155,156]	High toxicity level
			Poly(L-lactic acid-*co*-e-caprolactone) (P(LLA-CL)[74]	Good mechanical properties	Poor biocompatibility
			PGA[99,157]	Strong hydrophilicity Fast degradation	Poor cell attachment
			PLCL[99,157]	Reducing the inflammatory response Improve repair intensity Bio absorbability High elasticity Low cytotoxicity Controlled degradation Biocompatibility	Poor conductivity
			HA[100,108,111,119,150,158]	High biological activity Bone conductivity High compressive strength Low-cost[139,159–161]	Uncontrollable degradation rate Brittle failure Low porosity Low water absorption
			Graphene oxide (GO)[117]	Large specific surface area Numerous functional groups Excellent hydrophilicity Excellent mechanical properties[124,162,163]	Cytotoxicity
			Col[104,164]	Biodegradability Biocompatibility	Poor mechanical properties

Table 1 (*continued*)

Synthetic method	Fundamentals	Characteristics	Ingredients	Advantages	Drawbacks
Phase separation	Create porous polymer scaffolds by inducing the separation of a polymer solution into a polymer-poor phase and a polymer-rich phase[29]	Low-cost Small batch variation Achieve specific geometric shapes Limited raw materials available Lab-scale production Long and time consuming Difficult to control the structure stability	PLGA[39]	Biodegradability Biocompatibility	Poor mechanical properties Release of acidic by-products Low hydrophobicity Low biological activity
Self-assembly	Rely on noncovalent interactions to build nanofibers from small molecules, peptides, proteins and nucleic acids[29]	Produces smallest scale nanofiber Low productivity Complex processing High cost The generated nanofibers are less mechanical	PCL[165,166]	Biodegradable Easy processing	Poor biomechanical properties

fibrocartilaginous enthesis in some ways, there are still limitations. Fortunately, the use of nanofibrous scaffolds can compensate for their shortcomings to some extent, showing great potential in the field of promoting fibrocartilaginous enthesis healing.

The first implant to be cleared by the FDA, a synthetic nanofibrous scaffold (Rotium™; Atreon Orthopedics) made by poly(L-lactide-*co*-caprolactone) (PLCL) and PGA, can be used in conjunction with suture anchors for the reattachment of tendon to bone in RCR. The scaffold has an ECM biomimetic structure, which contributes to a likely mechanism that promotes a healing response similar to natural tissue.[97–99] During the operation, doctors insert absorbable nanofibrous scaffolds into the suture line between the bone and tendon, and use double-row repair technology to insert nanofibrous scaffolds between the bone and tendon.[99] When the inner end of the fibrocartilage is broken, the Rotium™ scaffold can promote its healing and improve its strength. Meanwhile, as a synthetic scaffold, it can decrease inflammatory reaction and cause less scarring at the fibrocartilaginous enthesis than biological scaffolds.[99] In a rabbit model of anterior fork ligament injury, the researchers wrapped biomimetic nanofiber membranes around autologous hamstring tendons. Eight weeks after surgery, they found that the biomimetic nanofibrous membrane formed new bone tissue between the tendon and bone, possibly because its biodegradable nanofibrous membrane facilitated the penetration of bone tissue into the fibrocartilaginous enthesis and promoted bone formation. In addition, the maximum failure load and failure stiffness were significantly higher at 8 weeks than in the control group.[100] In a small retrospective study, patients who used nanofibrous scaffolds to enhance RCR had significant improvements in the joint range of motion and functional outcome scores at an average of 10.5 months, with a cure rate of 91%.[99,101] Therefore, nanofibrous scaffolds are convenient to use during the operation and can effectively enhance the mechanical properties of postoperative fibrocartilaginous enthesis, thereby promoting the healing of the fibrocartilaginous enthesis and improving the functional outcome. Thus the use of nanofibrous scaffolds in clinical surgery shows promising therapeutic potential.

The application of nanofibrous scaffolds offers a good solution to solve non-surgical treatment problems. Nanofibrous scaffolds have a high aspect ratio surface area and good permeability and porosity, hence making them customizable to resemble the natural ECM.[102] This is beneficial for cell adhesion, proliferation, and differentiation.[103] By modifying the surface structure and chemical properties of the nanofibrous scaffold, it can encourage its positive interactions with cells and play a better role in promoting osteogenesis.[104] In contrast to PRP, nanofibrous scaffolds can be made to suit people's needs, and the quality of nanofibrous scaffolds can be controlled, both in terms of mechanical properties and biodegradability.[105,106] For example, nanofibrous scaffolds made from natural polymers have good biosafety, as they degrade slowly during tissue recovery without the production of toxic metabolites. Nanofibrous scaffolds made from synthetic polymers have a stable

chemical structure and controlled physicochemical properties. There are also composite nanofibrous scaffolds combining natural and synthetic polymers that can have excellent mechanical properties and ensure biosafety.[107] The nanofibrous scaffold can also mimic the ECM structure, tightly fit the fibrocartilaginous enthesis, and promote the healing of the whole enthesis.[108]

In summary, the nanofibrous scaffold has the advantages of easy preparation, wide source of raw materials, easy adjustment and easy modification, can mimic the natural structure and morphology of the fibrocartilaginous enthesis, and has good biocompatibility; all these advantages can compensate to a certain extent for existing surgical and non-surgical treatments and be combined with them to promote the repair of fibrocartilaginous enthesis.

4.1 Nanofibrous scaffolds with controllable morphology

The composition and structure of the fibrocartilaginous enthesis show gradient changes, which is conducive to smooth stress transfer.[51,109] Therefore, it is important to simulate the graded transition. At present, nanofiber scaffolds can promote the recovery of mechanical properties and regeneration of fibrocartilaginous enthesis by changing the morphology, such as fiber arrangement, and mineral content (Fig. 3a).[110–112] A summary of the composition, synthetic methods, regulatory mechanism, and function about nanofibrous scaffolds with controllable morphology are presented in Table 2.

The controllable morphology of nanofiber scaffolds is beneficial to promote the regeneration of fibrocartilaginous enthesis.[113] Therefore, some scholars have simulated the gradient mineralization of the fibrocartilaginous enthesis by photothermal welding to transform the nanofibers into nanofiber scaffolds with random gradient structures.[96] The temperature of the stent surface is positively correlated with the irradiation time. Under the same irradiation time, the higher the laser intensity, the faster the temperature increase of the stent surface. In the case of the same laser intensity, the higher the indocyanine green (ICG) content, the shorter the time to reach the surface temperature of the stent.[114] Researchers have set the irradiation times to 0, 5, 8, and 10 s to Orient the nanofiber arrangement from uniaxial to random (Fig. 3b). Then, the polyurethane (PU) fiber film was immersed in simulated body fluid (SBF) at 0, 0.5, 1, and 2 h later to form a mineralization gradient (Fig. 3c). Regions I, II, III, and IV represent irradiation with 2 W cm^{-2} for 0, 5, 8, and 10 s. For the cells on the scaffold in the photothermal welding (PW) plus graded mineralization (PW + GM) group, the ratio of tendon-derived stem cells (TDSCs) (length to width) in region I was 3.3-times greater than in region IV. In the case of PW, the ratio was 2.8 times greater than in region IV, but there was no significant change in cell proliferation between the two groups (Fig. 3d). Fluorescence fiber images showed high expression of Tenascin C protein and low expression of Runt-related transcription factor 2 (Runx2) protein in region I (uniaxial arrangement), and high expression of Runx2 gene and low expression of Tenascin C in region IV (random arrangement) (Fig. 3e). This suggests that this double-gradient nanofiber scaffold promotes tendinogenic differentiation of TDSCs in region I and osteogenic differentiation in region IV. Masson's trichome staining after 3 and 6 weeks of implantation of the double gradient nanofiber scaffold found obvious damage in each group at the third week (Fig. 3f). The PW + GM group produced more connective tissue at the sixth week than the control group, and obvious chondroid tissue hyperplasia could be observed. Therefore, regulated nanofiber scaffolds are beneficial to guide cell osteoblastic or tendinogenic differentiation, thereby promoting the regeneration of fibrocartilaginous enthesis. Similarly, Jiang *et al.* distributed bone morphogenetic protein 2 (BMP-2) and nanohydroxyapatite (nanoHA) gradients on the nanofiber scaffold with fiber orientation from random to gradually arranged,[111] effectively guiding the morphology of bone marrow stem cells (BMSCs) from disordered to arranged. The region with high mineral content promoted the maturation of osteoblast phenotype, which may be conducive to the regeneration of fibrocartilaginous enthesis.

In addition, the adjustable nanofibrous scaffolds are beneficial to improve the mechanical properties of the fibrocartilaginous enthesis.[115] Therefore, Chen *et al.* manufactured a gradient mineral silk fibroin (GSF) nanofibrous scaffold with an SBF gradient coating in which the L region of GSF is immersed in SBF for the shortest time and therefore has the least mineral content, the M region contains a moderate amount of SBF, and the H region is immersed in SBF for the longest time and has the most mineral content (Fig. 4a).[116] Fig. 4b shows the gradual thickening of mineral layers from zone L to zone H. Histological staining shows that the organism has good biocompatibility after 8 weeks of implantation and produces a continuous transition zone (Fig. 4c). The GSF group (10.61 ± 0.83 N) was significantly stronger than the other groups (Fig. 4d and e). Therefore, this gradient mineralization of nanofiber scaffold significantly improves the mechanical energy of the adhesion point of fibrous cartilage, which is beneficial to the consolidation of tendon and bone. In addition to using SBF coating, graphene oxide (GO) can also be evenly distributed on nanofiber scaffolds.[117] In addition to using SBF coating, graphene oxide can also be evenly distributed on nanofiber scaffolds. This highly interconnected GO-PLGA nanofiber film has high porosity (Fig. 4f). Hematoxylin-eosin (H & E) staining analysis showed that GO-PLGA staining was gradually arranged regularly (Fig. 4g), while the control group still showed granuloma staining. Metachromasia staining analysis showed that GO-PLGA staining generated more cartilage tissues at the 12th week (Fig. 4h). Most importantly, the ultimate load and stress values between the supraspinatus tendon and humerus in the GO-PLGA group were significantly higher than those in the control group. Therefore, the controllable morphology of nanofiber scaffolds can not only achieve regeneration of fibrocartilage attachment sites but also significantly improve its biomechanical properties. In addition, nanofibrous scaffolds mixed with microfibers can also improve the mechanical properties of the fibrocartilaginous enthesis.[118] The scaffolds with PCL microfibers and PLGA nanofibers were prepared

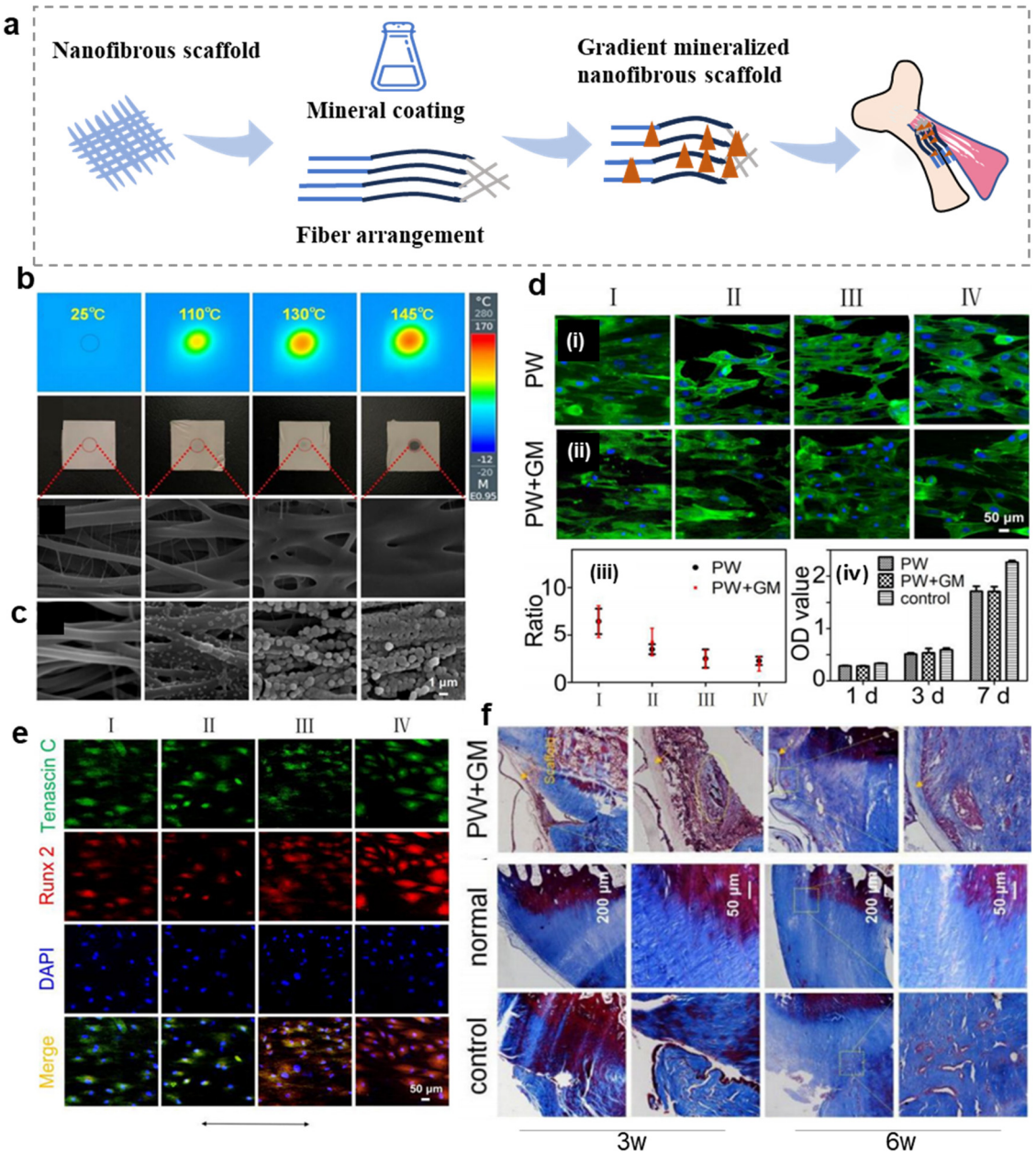

Fig. 3 Nanofibrous scaffolds with adjustable morphology can promote the regeneration of fibrocartilaginous enthesis. (a) Schematic diagram of a morphologically adjustable nanofibrous scaffold. (b) Polyurethane (PU)/indocyanine green (ICG) nano-scaffold infrared images, photographs, and SEM images show the surface temperature and morphology of nanofibrous scaffolds containing 1% ICG after exposure to lasers 0, 5, 8, and 10 s (from left to right) at 2 W cm^{-2} irradiance. (c) SEM images showing the corresponding nanofibrous scaffolds treated with mineralization solution for 0, 0.5, 1, and 2 h. (d) Fluorescence micrographs showing the morphologies of tendon-derived stem cells (TDSCs) after co-culture with the nanofibrous scaffolds treated by photothermal welding (PW) or photothermal welding plus graded mineralization (PW + GM) for 3 days. The plain glass was used as a control group. The arrow represents the direction of nanofiber orientation. The ratio of length and breadth of TDSCs incubated on different regions of the PW and PW + GM groups. The proliferation of TDSCs on the different samples tested by CCK-8 assay at 1, 3, and 7 days. (e) Tenogenic and osteogenic differentiation of the TDSCs on the different regions of the dual gradient scaffold. Fluorescence micrographs showing the expression of Tenascin C and Runx2 of TDSCs after co-culture with the nanofibrous scaffold treated by photothermal welding plus graded mineralization for 2 weeks. Cell nuclei are stained by DAPI. The arrow represents the direction of nanofiber orientation. (f) Masson staining at 3 and 6 weeks of implantation. Abbreviations: PW + GM, the photothermal welding plus graded mineralization group; PW, photothermal welding group. Fig. 3b–f have been reproduced from ref. 96 with permission from Springer Nature, copyright 2022.

using the interleaved electrospinning method, which significantly improved the strength and failure strain and stiffness of the torn tissue.[119]

In conclusion, the morphology of nanofibrous scaffolds can be easily changed to promote the regeneration of fibrocartilaginous enthesis and improve their mechanical properties.

Table 2 A summary of the composition, synthetic methods, regulatory mechanism, and function about nanofibrous scaffolds with controllable morphology

Composition	Synthetic methods	Regulatory mechanism	Function	Ref.
PLGA, BMP-2/nano HA, TGF-β3	Electrospinning technology	The contents of BMP-2 and nano HA were distributed in gradient, the fiber orientation was random to arrange, induce calcium and phosphorus deposition	Promote the zonal differentiation of BMSC to achieve the regeneration of fibrocartilaginous enthesis	111
PCL	Electrospinning technology	''Random-aligned-random'' fiber arrangement, (5× SBF) coating	Induce tendon formation and osteogenesis, guide collagen alignment, and have good tensile stress	113
PLGA	Electrospinning technology	Controlling the swelling and welding degree of the nanofibers in the nonwoven mat generates a gradient porosity and arrangement	The cell morphology of BMSCs was guided from uniaxial to random arrangement, simulating the structural organization of fibrocartilaginous enthesis	167
PCL, Col I, polydopamine (PDA)	Electrospinning technology	Col I and PDA were added to enhance biological activity	Promote the adhesion, proliferation, and differentiation of TSCs and promote bone formation	148
PLGA, dichloromethane (DCM), dimethylformaldehyde (DMF)	Electrospinning technology	Gradient content of 10× SBF	Promote osteogenic differentiation of ASCs	112
PCL, DCM, DMF	Electrospinning technology	The random fibers were deposited on a single drawn aligned nanofiber pad to form a fiber gradient	Simulating the arrangement of collagen fibers at the fibrocartilaginous enthesis	110
S10× simulated body fluid (SBF), silk fibroin (SF)	Electrospinning technology	Gradient content of 10× SBF	Enhance the integration of fibrocartilaginous enthesis, improve mechanical properties and promote fibrocartilage formation	116
PLLA, HA	Phase separation	The anisotropic and isotropic porosity was formed by freeze-drying method	Simulating the arrangement of collagen fibers at the fibrocartilaginous enthesis	108
PLGA, SBF	Electrospinning technology	Gradient content of 10× SBF	Improve the mechanical properties	115
PCL, chitosan (CS)	Electrospinning technology	Stagger-electrospun PCL microfibers and CS nanofibers	Improve the mechanical properties	118
PEUU, gelatin, 1,1,1,3,3,3-hexafluoro-2-propanol	Electrospinning technology	Used a multi-bonding network densification strategy	With bionic structure and tensile properties, promote cartilage differentiation	38
PU, ICG, hexafuoroisopropanol (HFIP)	Electrospinning technology	A random gradient structure is formed by the time formation of the photothermal welding technique, and a mineralization gradient is formed by the time of immersion in the SBF	Improve tendon tension and promote Col I formation	96
GO, PLGA	Electrospinning technology	Add GO to reduce diameter and improve porosity	Promote bone and cartilage formation, improve collagen alignment and mechanical properties.	117
PLGA, ethyl alcohol, *N*,*N*-dimethylformamide	Electrospinning technology	Used custom rotating mandrel to produce aligned fiber arrangement	Directs fibroblast attachment, gene expression, and matrix deposition	168
PLGA, HA, heparin	Electrospinning technology	Gradient content of 10 × SBF	Improve mechanical properties	169
PLLA-CL, SF, HFIP	Electrospinning technology	A rotating drum collector is applied at a rate of 3000 rpm to form an array of nanofibers on the random nanofibers	Induce bone and fibrochondrogenesis, improve collagen tissue and maturity, enhance tendon and bone integration, and improve gradient microstructure	74
PLGA, HA, BMP-2	Electrospinning technology	Gradient content of HA and BMP-2, PLA microfibers were added	Improve mechanical properties and induce cartilage formation	119

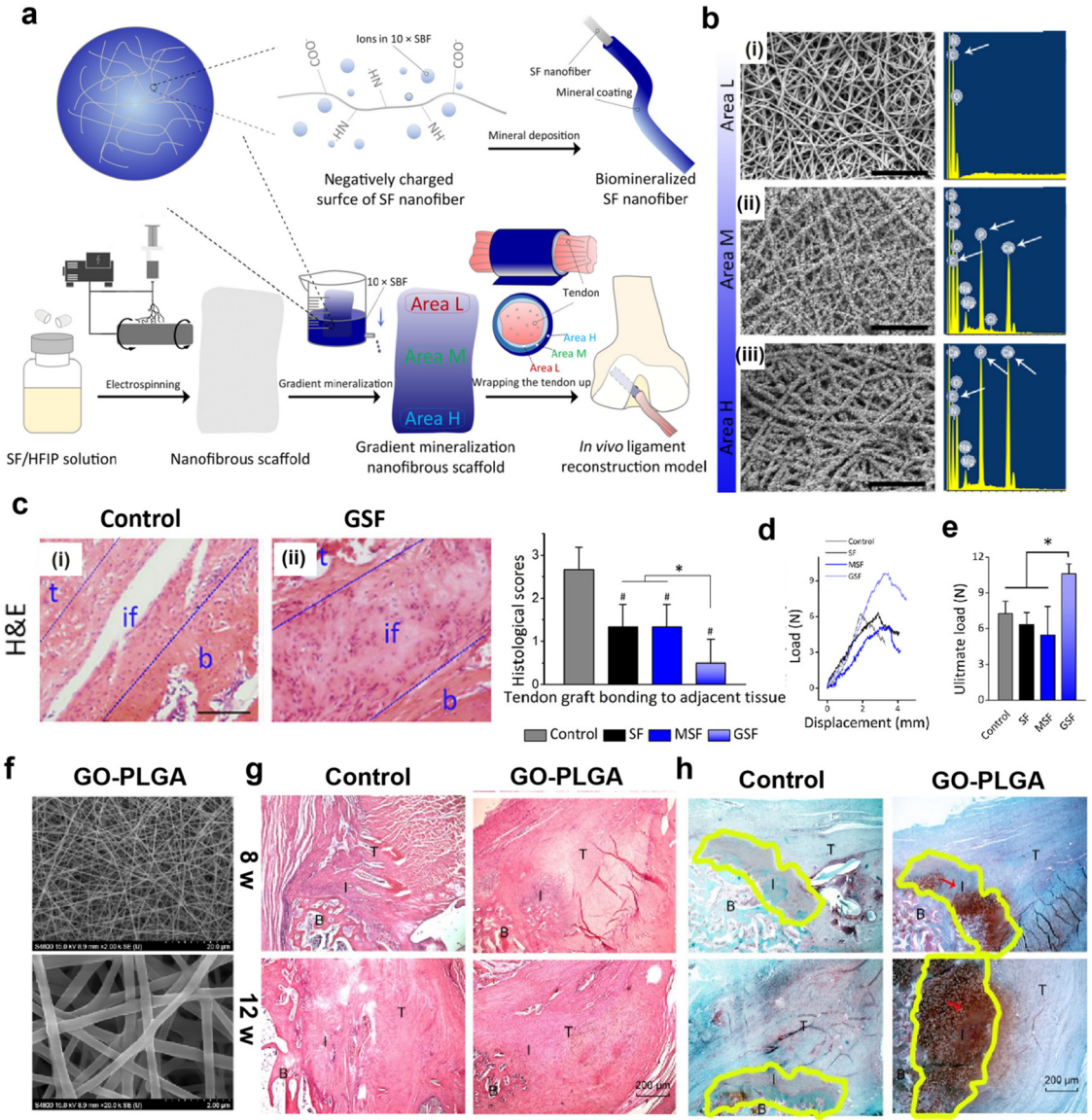

Fig. 4 Nanofibrous scaffolds with adjustable morphology can improve mechanical properties and regeneration of fibrocartilaginous enthesis. (a) Schematic illustration of fabrication of a gradient mineralization SF scaffold for integration of tendon to bone interface in a rat model. Areas L, M, and H represent low, medium, and high mineralization levels, respectively. (b) The SEM images and corresponding energy spectra of region L, region M, and region H of the gradient scaffold. Scale: 10 μm. (c) HE staining tissue sections of the tendon-to-bone interface 8 weeks after surgery. Histological analysis of the representative hematoxylin and eosin-stained tissue section of the tendon-to-bone interface. #$p < 0.05$, compared with the control group; *$p < 0.05$. Data presented are in the form of mean ± SD; scale bar: 100 μm. t, tendon; if, interface; b, bone. (d) Representative load displacement curves for biomechanical tests of tendon bone integration and (e) ultimate loads of control, SF, and GSF groups at 8 weeks post-surgery. *$p < 0.05$. Data are presented as mean ± SD. Fig. 4a–e have been reproduced from ref. 116 with permission from the American Chemical Society, copyright 2021. (f) Scanning electron microscope image of GO-PLGA nanofibrous membrane (g) Representative H & E-stained tissue sections (40×) of the supraspinatus tendon insertion site at 4 and 8 weeks postoperatively. (h) Representative histology images of the cartilage tissue at the insertion. Abbreviations: SBF, simulated body fluid; SF, silk fibroin; HFIP, hexafluoroisopropanol; GO, graphene oxide; PLGA, poly (lactic-*co*-glycolic acid). Fig. 4f–h have been reproduced from ref. 117 with permission. International Journal of Nanomedicine, 2019, **14**, 1835–1847 Originally published by, adopted, and used with permission from Dove Medical Press Ltd.

4.2 Nanofibrous scaffolds for controlled release of drugs

Following damage to the enthesis, immune cells produce excessive amounts of ROS during the inflammatory stage of the healing pathway, inducing oxidative damage and causing chronic inflammation and fibrosis at the interface, leading to excessive scar tissue formation. In contrast, inhibition and clearance of excess ROS can accelerate the transition from the inflammatory phase to the later healing phase, which is important for alleviating local inflammation and promoting tissue regeneration.[120,121] Nanofibrous scaffolds have shown more advantages in controlling drug release because of the characteristics of low dose and sustainable release of drugs

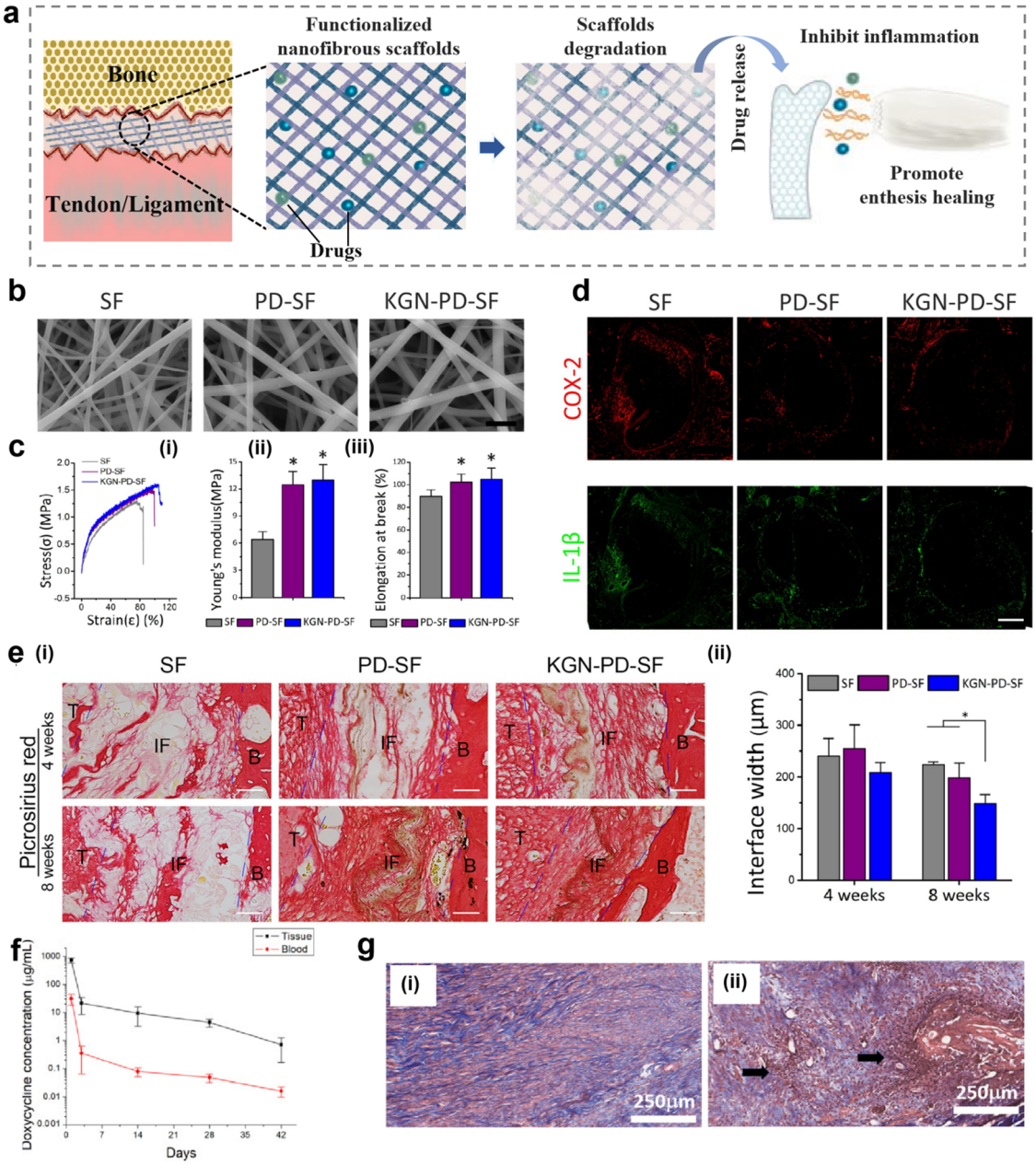

Fig. 5 Nanofibrous scaffolds for controlled release of drugs. (a) A schematic illustration of a nanofiber scaffold that can be modified to achieve effective loading and on-demand release of drugs, improving inflammatory responses. (b) Scanning electron microscope (SEM) image of modified nanofibrous scaffold. Bars represent 2 μm. (c) Characteristics of modified nanofibers (KGN-PD-SF). (i) Strain–stress curve of KGN-PD-SF. (ii) Young's modulus of KGN-PD-SF. (iii) Elongation at breaking of KGN-PD-SF. (d) Representative immunofluorescence images of inflammatory markers (COX-2 and IL-1β) in bone tunnels in the SF, PD-SF, and KGN-PDSF groups 1 week after surgery. Scale bar: 200 μm. (e) Histological characterization of the SF group, PD-SF group, and the KGN-PD-SF group at 4 and 8 weeks after surgery. Bars represent 50 μm. (i) Results of picrosirius red staining evaluation of the SF group, PD-SF group, and the KGN-PD-SF group at 4 and 8 weeks after surgery. Images observed under normal conditions. (ii) Interface width analysis with H & E-stained slides. Fig. 5b–e have been reproduced from ref. 37 with permission from Elsevier, copyright 2022. (f) *In vivo* release of doxycycline in tissues and blood over time. (g) H&E staining of the Achilles tendon at 4 weeks post-surgery. (i) Doxycycline group (ii) control (surgery only, no membrane) group. (Magnification: ×160, Pink represents collagen fiber. Arrow: white blood cell accumulation indicating inflammation). Abbreviations: PD, polydopamine; KGN, kartogenin; SF, silk fibroin; COX-2, cyclooxygenase-2; IL-1β, interleukin -1 beta; B, bone; IF, interface; T, tendon. H&E, hematoxylin and eosin. Fig. 5f and g have been reproduced from ref. 124 with permission from MDPI.

supported by nanofibrous scaffolds, thus minimizing systemic side effects.[122,123]

Nanofibrous scaffolds can be surface modified to achieve effective loading and on-demand release of drugs to scavenge ROS and improve the inflammatory response (Fig. 5a). Therefore, a multifunctional nanofiber scaffold with antioxidant function and promotion of fibrocartilage formation was prepared by polydopamine (PD) modification and kartogenin

(KGN) carboxylation reaction on the surface of silk nanofibers.[37] The morphology of the modified nanofibrous scaffolds was analyzed by scanning electron microscopy (SEM). The results showed that the nanofibrous scaffolds form a porous network with an ECM-like structure (Fig. 5b). The mean diameter of the modified nanofibers increased and they exhibited better tensile properties, higher Young's modulus, and elongation at breaking (Fig. 5c). In addition, the implantation of multifunctional nanofiber scaffolds into rats with ACL injuries was effective in reducing the inflammatory response induced by oxidative stress *in vivo*. The inflammatory response at the interface was analyzed by immunofluorescence staining for cyclooxygenase-2 (COX-2) and IL-1β. A significant decrease in the local inflammatory response in the bone tunnel of the PD-silk fibroin (SF) group and KGN-PD-SF group at 1 week after surgery could be observed (Fig. 5d). The analysis of picrosirius red staining at 4 and 8 weeks after surgery showed that the collagen organization in the KGN-PD-SF group was significantly more than that in others, and oriented collagen fibers could be seen at 8 weeks. At the same time, the interface width of the KGN-PD-SF group was significantly smaller than that of other groups at 8 weeks, which indicated better integration (Fig. 5e).

For the same purpose, PLGA nanofiber pads doped with doxycycline were prepared and evaluated *in vivo* using a rabbit model.[124] As shown in Fig. 5f, this PLGA nanofiber pad provides continuous release of doxycycline for more than 42 days *in vitro*. In addition, doxycycline was released in tissues and blood over time, and the systemic drug concentration was significantly lower *in vivo*. Furthermore, H & E staining performed 4 weeks after implantation of the PLGA nanofiber pad showed that the tendon cells in the doxycycline group were mature and lined up, while those in the control group without the nanofiber pad had a large accumulation of white blood cells and a significant inflammatory response (Fig. 5g). Therefore, the drug-loaded nanofiber pad effectively controls the inflammatory response and can be released continuously and in low doses. To control inflammation and promote tissue regeneration, loading inflammation-responsive prodrugs onto nanofiber scaffolds is also a good choice.[123] Chronic inflammation greatly inhibits the repair or regeneration of tissues. Therefore, Ye *et al.* constructed nanofiber-based scaffolds that can regulate chronic inflammation by releasing anti-inflammatory drugs in response to the occurrence of inflammation. *In vitro* studies have shown that the inflammation-responsive nanofiber scaffold can effectively inhibit the cytokines secreted from RAW264.7 macrophage cells, which indicated that nanofibrous scaffolds have great potential in regulating chronic inflammation in tissue regeneration.[125]

Nanofiber scaffolds can not only load anti-inflammatory drugs but also carry some small molecule drugs to induce the regeneration of fibrocartilaginous enthesis.[126] Zhu *et al.* encapsulated KGN in an array of nanofibers to prevent it from spreading to other areas. Studies have shown that the biological effects of KGN can be maintained for 20 days, and the nanofiber membrane extends the action time of KGN.

In short, the nanofibrous scaffold is an excellent biomaterial. Nanofiber scaffolds have the characteristics of low dose, extending release time, and minimizing systemic side effects. Therefore, nanofiber scaffolds show certain advantages in controlled release of drugs.

4.3 Stimulus-responsive nanofibrous scaffolds

In recent years, with the increasing demand for precision medicine and personalized medicine therapy, materials with stimulus-response characteristics have attracted widespread attention. Stimulus-responsive materials can respond to electrical and ROS signals and produce physical and physiological changes.[127] Compared with other polymer fibers or nanoparticles, electrospinning fibers with stimulation response characteristics have high sensitivity and response rate due to their high surface-volume ratio, high porosity, and easy adjustment.[128] They can play their role by communicating with the environment, and nanotechnology allows them to have a high surface-to-volume ratio, which can effectively sense changes in the surrounding environment. After passing through the nanofibers made by electrospinning technology, the stimulation is accelerated, resulting in a faster response owing to the nanofibers' small diameter, large surface area-to-volume ratio, and highly porous structure. Various types of stimulus-responsive nanofibers have been applied to musculoskeletal system repair; hence, they are likely promising targets for the healing of fibrocartilaginous enthesis (Fig. 6a).[129]

Electrical stimulation is one of the most commonly used stimuli.[128] Recently, it has been found that Col I in tendon has piezoelectric properties, which has prompted people to conduct in-depth research on the role of bioelectricity in tissue repair.[130,131] A synthetic compliant ferroelectric polymer (PVDF-TrFE) was integrated into a nanofiber scaffold with electrical, mechanical, and morphological properties of Col I to simulate the bioelectrical signals provided by collagen piezoelectricity to maintain the tendon cell phenotype and promote tendon regeneration (Fig. 6b).[129] To simulate the layered structure of the tendon collagen fibers, the collector velocity was controlled between 4.2 m s^{-1} and 29.3 m s^{-1} (Fig. 6c). The scaffolds obtained under the condition of 29.3 m s^{-1} had a highly organized fiber morphology, while those obtained under the condition of 4.2 m s^{-1} had a wider distribution of oriented fibers. Because of the geometric boundary variables that control the piezoelectric response of a single PVDF-TrFE fiber, the fibered piezoelectric scaffold exhibits higher piezoelectric properties than the piezoelectric film (Fig. 6d). When tendon-derived cells were inoculated on the commercial PVDF-TrFE membrane with lower piezoelectric coefficient and the piezoelectric nanofiber scaffold with the highest piezoelectric coefficient and fiber alignment (Fig. 6e), it was evident that the piezoelectric nanofiber scaffold with high fiber orientation and piezoelectric coefficient improved the gene expression of Scleraxis (Scx) and Tenomodulin (Tnmd). Previous studies have shown that tendon stem cell differentiation can enhance the expression of Scx and Tnmd, thereby promoting the healing of fibrocartilaginous enthesis.[132] At the same time, transcription

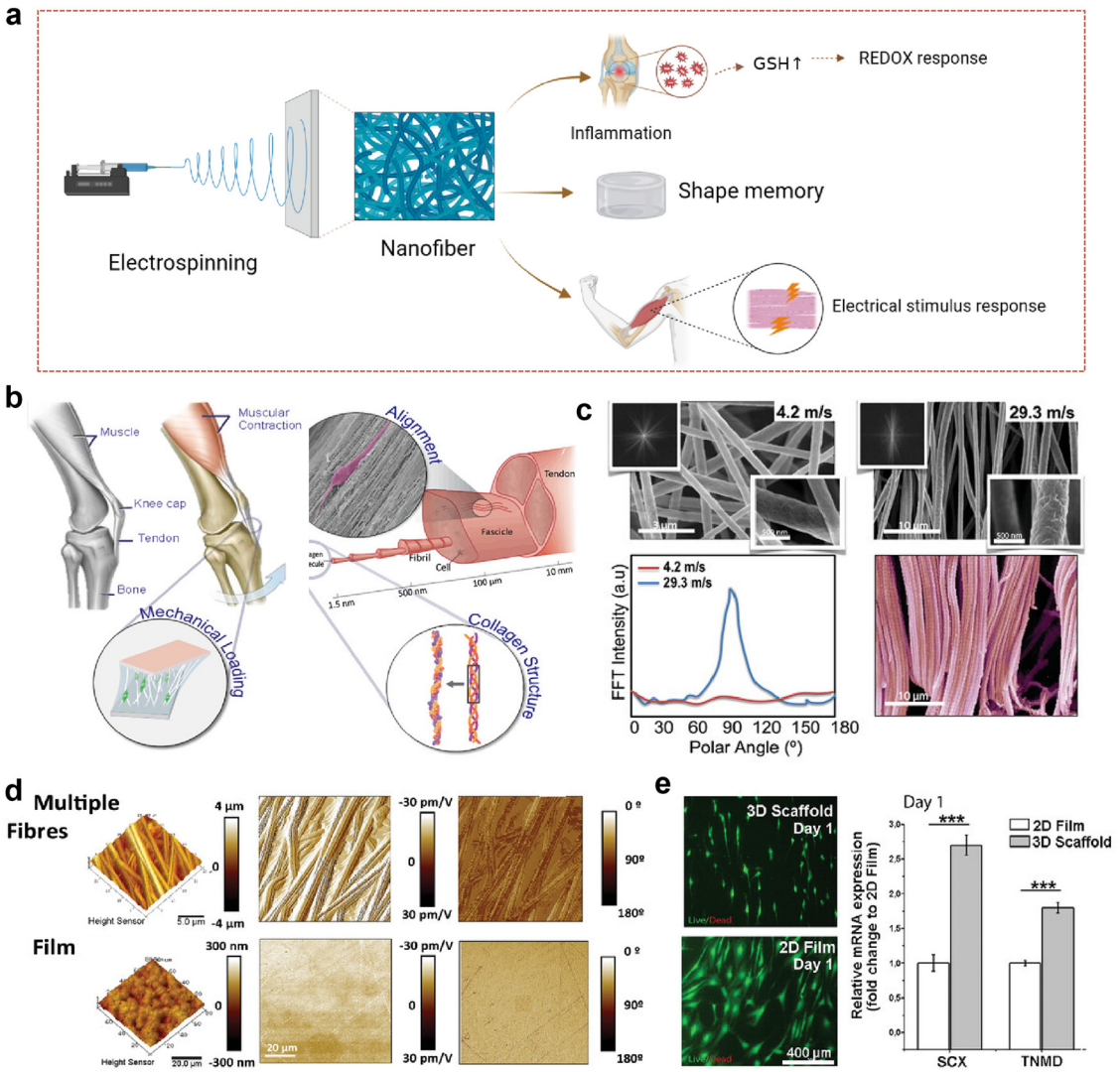

Fig. 6 Nanofibrous scaffolds in response to electrical stimulation. (a) A schematic illustration of a nanofiber scaffold that can be modified to achieve effective loading and on-demand release of drugs, improving inflammatory responses. This figure was created with BioRender.com. (b) Schematic diagram of activation of tendon specific regeneration pathway by piezoelectric derived electric field generated during physiological movement. (c) Scanning electron microscope (SEM) image of modified nanofibrous scaffold. (d) The morphology of scaffolds obtained by electrospinning collected at low (4.2 m s^{-1} rpm) and high (29.3 m s^{-1}) linear speeds. Fast Fourier transform (FFT) spectra showed a broad distribution of intensities for low speed (4.2 m s^{-1}) and a clear peak for high speed (29.3 m s^{-1}), characteristic of highly anisotropic structures. (d) PFM amplitude and phase images for a piezoelectric scaffold and film. (e) Cells demonstrated differential expression of tenospecific proteins and morphological changes when cultured on electrospun scaffolds or planar PVDF-TrFE films. hTDCs maintained their phenotype and expression levels of TNMD and Scx when cultured on aligned piezoelectric scaffolds; this effect was absent on 2D planar films ($N = 3$, $r = 3$, mean ± SD, $***p < 0.001$). Abbreviations: GSH, glutathione. Fig. 6b–e have been reproduced from ref. 129 with permission from Wiley-VCH, copyright 2021.

factor Scx plays an important role in the development and maturation of fibrocartilaginous enthesis.[133] Histological staining analysis of Scx-knocked out (cKO) mice and wild-type (WT) mice on day 56 after birth showed that the lumen of mature cKO was full of round chondrocyte-like cells, and there were no obvious wet marks compared with WT, suggesting that the fibrochondral lumen of cKO mice was damaged because of maturation. The stress–strain curve from uniaxial tensile test to failure of the supraspinicular fibrocartilaginous enthesis of WT and cKO mice, and the final failure strength of WT mice is higher than that of cKO mice. The fibrocartilaginous enthesis of WT mice have better biomechanical properties. Therefore, increasing the expression of Scx and Tnmd is beneficial to the healing of fibrocartilaginous enthesis. Moreover, piezoelectric nanofiber scaffolds have also been shown to increase the expression of Sox and Tnmd;[129] therefore, we speculate that piezoelectric nanofiber scaffolds may also promote the healing of fibrocartilaginous enthesis.

In addition, REDOX response is also one of the common stimulus responses.[128] It is well-known that ROS are produced during the inflammatory period of healing after tissue injury, which is one of the defense mechanisms of the human body

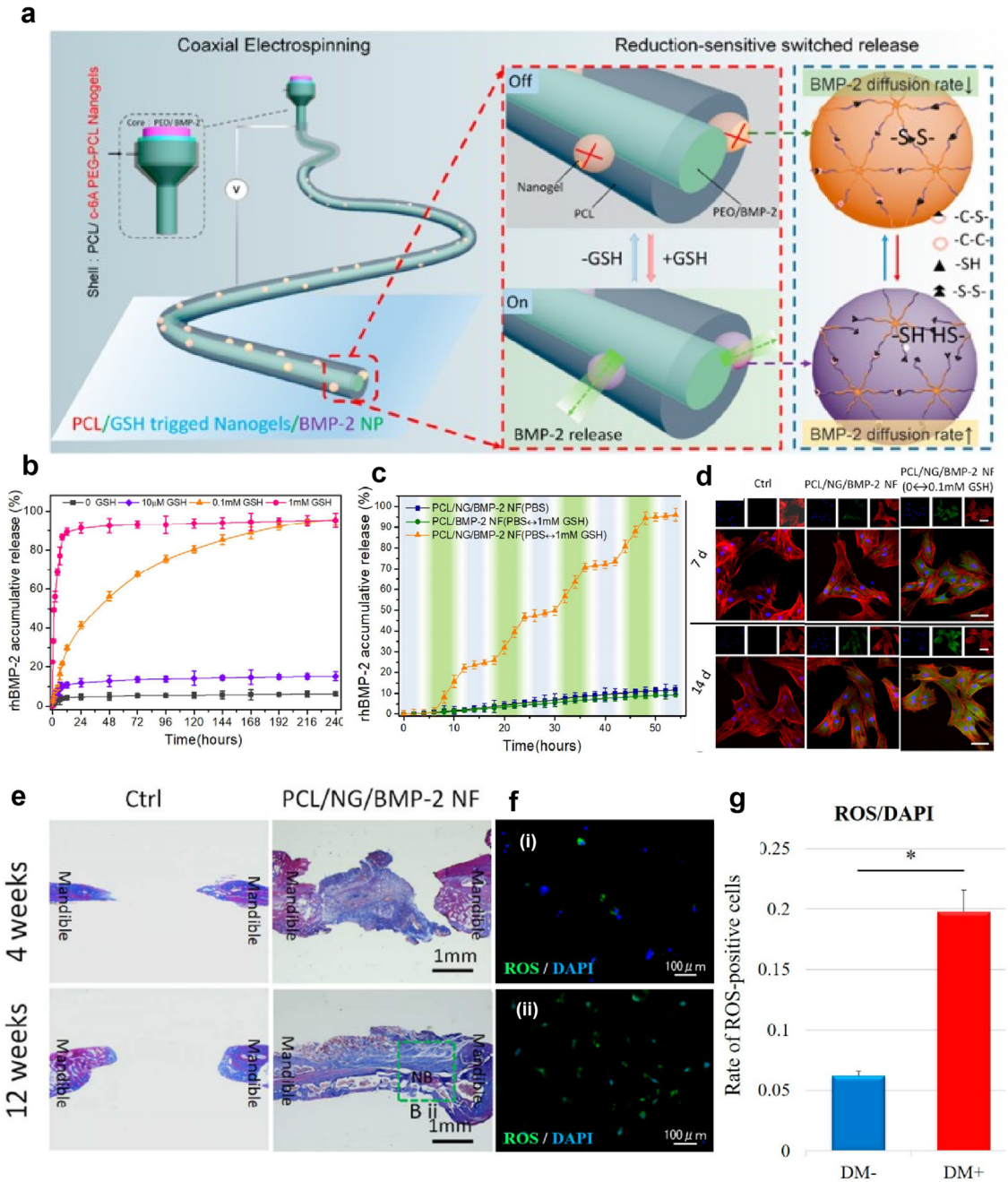

Fig. 7 REDOX-responsive nanofibrous scaffolds. (a) Schematic diagram of fabrication of REDOX-sensitive nanofibers. (b) REDOX-sensitive release behavior of nanofibers with different BMP-2 in different GSH contents at 37 °C. (c) The stepwise response of nanofibers on increasing GSH concentration at fixed intervals. (d) Confocal laser scanning microscope images of immunostained cellular components (merged) for the rBMSCs, stained for F-actin (red), OCN protein (green), and nuclei (blue) (Scale bar: 20 μm). These cells were also cultured at days 7 and 14 post seeding, respectively, on such surfaces as Control, PCL/NF/BMP-2 NF, and PCL/NG/BMP-2 NF (PBS ↔ GSH) with GSH at fixed intervals. (e) Histomorphometric results of the bone defect area (NB: New Bone). Fig. 7a–e have been reproduced from ref. 134 with permission from the American Chemical Society, copyright 2018. (f) Representative immunofluorescence images of ROS levels detected in rotator cuff derived cells: (i) non-diabetic controls and (ii) diabetic groups. DCFH–DA staining (green) is indicative of the accumulation of ROS in rotator-cuff-derived cells; the nuclei are counterstained with 4′,6-diamidino-2-phenylindole (DAPI; blue). (g) Relative quantification of the ROS-positive cells. ROS-positive cells and DAPI-positive cells in four rectangular areas (0.75 mm × 1.0 mm) on each slide were counted and their mean values were analyzed. The ROS-positive cells rate (number of ROS-positive nuclei/DAPI-positive nuclei) is given as the mean of the four areas. Data are presented as the mean ± SD. The independent *t*-test was performed for determining significant differences: $*p < 0.001$. Abbreviations: ROS, reactive oxygen species; DAPI, 4,6-diamidino-2-phenylindole; PCL, polycaprolactone; GSH, glutathione; BMP-2, bone morphogenetic protein 2. Fig. 7f and g have been reproduced from ref. 135 with permission from MDPI, copyright 2022.

against foreign body invasion and pathogens.[120,121] Increased glutathione synthesis can be detected in the abnormal reactive oxygen microenvironment,[127] so it is feasible to detect the level of glutathione (GSH) as an oxido-reduced nanofiber scaffold. Gong *et al.* prepared a novel REDOX responsive drug-loaded nanofiber for bone reconstruction (Fig. 7a).[134] Polyethylene oxide (PEO) and BMP-2 form the inner core region, and a mixture of PCL and redox reaction c-6A PEG-PCL nanogels form the shell. Fig. 7b shows the BMP-2 release curve of core–shell nanofibers in response to different concentrations of GSH in PBS. After incubation for 48 h, 10 μM, 0.1 mM, and 1 mM GSH released 13 ± 1.5, 55 ± 2.5, and 90 ± 2.9% of BMP-2, respectively, while only 3% BMP-2 was released in the group without GSH, indicating that the core–shell nanofibers had good oxidation-reducing properties. To demonstrate the oxidative switch release behavior of the nanofibers, they used an ELISA instrument to monitor the amount of BMP-2 released (Fig. 7c). It can be found that the concentration of BMP-2 increases sharply at 0.1 mM GSH and only slightly in PBS, suggesting that the release triggered by oxygen reduction is adjustable. Subsequently, immunofluorescence staining was used to detect the osteoblast differentiation of MSCs *in vitro* by oxidation-sensitive nanofibers releasing BMP-2, and the expression of osteocalcin (OCN) was used as a marker for detecting osteoblast differentiation (Fig. 7d). The OCN expression of the PCL/nanogels (NG)/BMP-2 NF and PCL/NG/BMP-2 NF (PBS ↔ GSH) group was significantly increased compared with the control group, while the OCN expression level of the PCL/NG/BMP-2 NF (PBS ↔ GSH) group was the highest. This suggests that the REDOX-sensitive nanofibers can promote osteogenic differentiation of MSCs *in vitro*. Histological analysis of the *in vivo* osteogenic ability of oxidation sensitive nanofibers in the mandibular defect repair was performed (Fig. 7e). Compared with the control group, the PCL/NG/BMP-2 NF group had new bone formation near the defect side. Thus, this REDOX-sensitive nanofiber scaffold controls the release of BMP-2 by responding to GSH levels in ROS. Intracellular ROS levels in patients with rotator cuff tear were measured by DCFH-DA staining and quantitative analysis of ROS-positive cells (Fig. 7f and g).[135] The results showed that diabetic patients with rotator cuff tears had high levels of ROS. Therefore, we speculate that REDOX-responsive nanofiber scaffolds may also contribute to the synthesis of GSH in ROS in diabetic patients with rotator cuff tears to release drugs and promote repair of the rotator cuff fibrocartilaginous enthesis.

In addition to electrical stimulation response and reduction response, nanofibers also have shape memory, thermal response, pH response, and other characteristics.[128,136,137] Shape memory polymers are active materials that can remember permanent shapes through chemical or physical crosslinking.[138] Their shapes can be changed in a predetermined way under external stimuli, and their applications in medicine have attracted widespread attention. Electrospun nanofibers with shape memory characteristics have special response to temperature and are also suitable for remote or self-regulating drives.[136] At the same, it has good biocompatibility and flexibility and can regulate cell behavior, which is promising for surgical repair of fibrocartilaginous enthesis.[139,140]

In summary, the stimulation-responsive nanofibers have the characteristics of high specific surface area, high porosity, and adjustability, and can quickly perceive internal or external stimuli and make appropriate responses, which has potential application prospects in promoting the healing process of fibrocartilaginous enthesis.

5. Conclusion

Over the past two decades, nanofibers have been widely used in various biomedical fields.[141] To achieve perfect healing of the fibrocartilaginous enthesis, it is necessary to have a deep understanding of its structure and composition. However, at present, the healing mechanism of fibrocartilaginous enthesis is still unclear, such as the molecular mechanism of inflammation, proliferation, and remodeling period. A clear mechanism will help us to control the disease and alleviate the burden of musculoskeletal system diseases.

There are a variety of treatments to promote fibrocartilaginous enthesis, but they all have certain limitations. Nanofibrous scaffolds show potential in the field of nanotechnology. However, most current studies have used animal models to evaluate the repair effect, and there is still a long way to go before it can be used in the clinic, but only if the implantation of nanofibrous scaffolds is not harmful to humans.

The morphology of nanofibrous scaffolds can be changed by changing fiber arrangement, porosity, and mineral content. Simulating the morphology of fibrocartilaginous enthesis is conducive to improving mechanical properties and tissue regeneration. We are looking forward to more ways to change the morphology of nanofibrous scaffolds to promote the healing of fibrocartilaginous enthesis, and combining them with the advantages of various materials seems to be an option.

Nanofibrous scaffolds with controlled drug release have shown great potential in inhibiting early inflammation and regeneration of fibrocartilaginous enthesis. At present, artificial intelligence (AI) technology can analyze the distribution imaging and tissue imaging of drugs in the body,[142] and it may also be possible to use AI technology in the future to explore the characteristics of the distribution of controlled release drugs in the human body with nanofiber scaffolds.

The application of stimulus-responsive nanofibrous scaffolds in the musculoskeletal system has led us to speculate the possibility of their use in fibrocartilaginous enthesis. Our current literature is limited to electrical response, REDOX response, and shape memory, and more types of stimulus response should be explored in the future. For example, pH-responsive nanofibers have received a lot of attention in drug delivery because they can trigger the release of drugs in inflammatory tissues or locally low pH environments in tumors.[143] Moreover, the pH of the fiber triggers drug release more superiority than that of the drug in the particle, but the specific mechanism is still not well understood.[144]

In conclusion, nanofibrous scaffolds have certain application prospects in promoting the healing of fibrocartilaginous enthesis, but further extensive research is still needed to realize its practical clinical application.

Conflicts of interest

There are no conflicts to declare.

Acknowledgements

This work was financially supported by the Key-Area Research and Development Program of Guangdong Province (2020B0-101020001), National Key R&D Program of China of Ministry of Science and Technology of China (2022YFC2409700 and 2022YFC2401804) and National Nature Science Foundation of China (31971318 and 22027810).

References

1 T. Lei, T. Zhang, W. Ju, X. Chen, B. C. Heng, W. Shen and Z. Yin, *Bioact. Mater.*, 2021, **6**, 2491–2510.
2 E. Pugliese, I. Sallent, S. Ribeiro, A. Trotier, S. H. Korntner, Y. Bayon and D. I. Zeugolis, *Mater. Today Bio*, 2023, **19**, 100584.
3 A. Sensini, G. Massafra, C. Gotti, A. Zucchelli and L. Cristofolini, *Front. Bioeng. Biotechnol.*, 2021, **9**, 645544.
4 S. Namdari, T. Nicholson, T. J. Brolin, J. Lu, J. A. Abboud and M. D. Lazarus, *J. Sports Med. Phys. Fitness*, 2021, **49**, 2042–2047.
5 S. Font Tellado, E. R. Balmayor and M. Van Griensven, *Adv. Drug Delivery Rev.*, 2015, **94**, 126–140.
6 N. Maffulli, J. Wong and L. C. Almekinders, *Clin. Sports Med.*, 2003, **22**, 675–692.
7 C. Yang, Y. Teng, B. Geng, H. Xiao, C. Chen, R. Chen, F. Yang and Y. Xia, *Front. Bioeng. Biotechnol.*, 2023, **11**, 1118468.
8 Q. Jiang, L. Wang, Z. Liu, J. Su, Y. Tang, P. Tan, X. Zhu, K. Zhang, X. Ma, J. Jiang, J. Zhao, H. Lin and X. Zhang, *Bioact. Mater.*, 2023, **20**, 1–15.
9 M. E. Steiner, M. M. Murray and S. A. Rodeo, *J. Sports Med. Phys. Fitness*, 2008, **36**, 176–189.
10 M. A. Fernandez-Yague, S. A. Abbah, L. McNamara, D. I. Zeugolis, A. Pandit and M. J. Biggs, *Adv. Drug Delivery Rev.*, 2015, **84**, 1–29.
11 A. Lee-Barthel, C. A. Lee, M. A. Vidal and K. Baar, *Transl. Sports Med.*, 2018, **1**, 60–72.
12 S. Patel, A. P. Gualtieri, H. H. Lu and W. N. Levine, *Ann. N. Y. Acad. Sci.*, 2016, **1383**, 97–114.
13 A. C. Colvin, N. Egorova, A. K. Harrison, A. Moskowitz and E. L. Flatow, *J. Bone Jt. Surg., Am.*, 2012, **94**, 227–233.
14 W. Luo, Y. Wang, Q. Han, Z. Wang, J. Jiao, X. Gong, Y. Liu, A. Zhang, H. Zhang, H. Chen, J. Wang and M. Wu, *J. Tissue Eng.*, 2022, **13**, DOI: **10.1177/20417314221144714**.
15 J. Zou, W. Yang, W. Cui, C. Li, C. Ma, X. Ji, J. Hong, Z. Qu, J. Chen, A. Liu and H. Wu, *J. Nanobiotechnol.*, 2023, **21**, 14.
16 D. Ma, Y. Wang and W. Dai, *Mater. Sci. Eng., C*, 2018, **89**, 456–469.
17 M. E. Ogle, C. E. Segar, S. Sridhar and E. A. Botchwey, *Exp. Biol. Med.*, 2016, **241**, 1084–1097.
18 T. Guan, J. Li, C. Chen and Y. Liu, *Adv. Sci.*, 2022, **9**, e2104165.
19 S. Han, Y. Liu, X. Nie, Q. Xu, F. Jiao, W. Li, Y. Zhao, Y. Wu and C. Chen, *Small*, 2012, **8**, 1596–1606.
20 Y. Liu, C. Chen, P. Qian, X. Lu, B. Sun, X. Zhang, L. Wang, X. Gao, H. Li, Z. Chen, J. Tang, W. Zhang, J. Dong, R. Bai, P. E. Lobie, Q. Wu, S. Liu, H. Zhang, F. Zhao, M. S. Wicha, T. Zhu and Y. Zhao, *Nat. Commun.*, 2015, **6**, 5988.
21 D. Sun, H. Wang, J. Liu, X. Wang, H. Guo, L. Xue, L. Li, J. Li, B. Zhang, Y. Xue, S. Li and Y. Liu, *Nano Today*, 2022, **44**, 101467.
22 X. Wang, W. Xu, J. Gu, X. Yan, Y. Chen, M. Guo, G. Zhou, S. Tong, M. Ge, Y. Liu and C. Chen, *Nanoscale*, 2019, **11**, 17782–17790.
23 S. Xu, C. Wang, R. Mao, X. Liang, H. Wang, Z. Lin, J. Li, S. Li, J. Jiang, T. Zhang, Y. Ma, Y. Liu, C. C. Han and Y. Liu, *Bioact. Mater.*, 2022, **12**, 16–29.
24 Y. Zhang, Y. Xue, Y. Ren, X. Li and Y. Liu, *Polymers*, 2023, **15**, 1566.
25 Z. Fu, Y. Zhuang, J. Cui, R. Sheng, H. Tomás, J. Rodrigues, B. Zhao, X. Wang and K. Lin, *Eng. Regener.*, 2022, **3**, 163–181.
26 Z. Luo, J. Che, L. Sun, L. Yang, Y. Zu, H. Wang and Y. Zhao, *Eng. Regener.*, 2021, **2**, 257–262.
27 Y. Zhu, B. Kong, R. Liu and Y. Zhao, *Smart Med.*, 2022, **1**, e20220006.
28 K. Qiao, L. Xu, J. Tang, Q. Wang, K. S. Lim, G. Hooper, T. B. F. Woodfield, G. Liu, K. Tian, W. Zhang and X. Cui, *J. Nanobiotechnol.*, 2022, **20**, 141.
29 R. L. Dahlin, F. K. Kasper and A. G. Mikos, *Tissue Eng., Part B*, 2011, **17**, 349–364.
30 A. Yusuf Aliyu and O. A. Adeleke, *Pharmaceutics*, 2023, **15**, 986.
31 X. Xie, Y. Chen, X. Wang, X. Xu, Y. Shen, A. u R. Khan, A. Aldalbahi, A. E. Fetz, G. L. Bowlin, M. El-Newehy and X. Mo, *J. Mater. Sci. Technol.*, 2020, **59**, 243–261.
32 H. Cao, T. Liu and S. Y. Chew, *Adv. Drug Delivery Rev.*, 2009, **61**, 1055–1064.
33 F. Huang, L. Cheng, J. Li and B. Ren, *Front. Bioeng. Biotechnol.*, 2022, **10**, 1078453.
34 S. Anjum, F. Rahman, P. Pandey, D. K. Arya, M. Alam, P. S. Rajinikanth and Q. Ao, *Int. J. Mol. Sci.*, 2022, **23**, 9206.
35 T. Yao, M. B. Baker and L. Moroni, *Nanomater.*, 2020, **10**, 887.
36 S. Zhu, Z. He, L. Ji, W. Zhang, Y. Tong, J. Luo, Y. Zhang, Y. Li, X. Meng and Q. Bi, *Front. Bioeng. Biotechnol.*, 2022, **10**, 897010.
37 P. Chen, S. Wang, Z. Huang, Y. Gao, Y. Zhang, C. Wang, T. Xia, L. Li, W. Liu and L. Yang, *J. Mater. Sci. Technol.*, 2021, **70**, 91–104.

38 L. Wang, T. Zhu, Y. Kang, J. Zhang, J. Du, H. Gao, S. Chen, J. Jiang and J. Zhao, *Bioact. Mater.*, 2022, **16**, 149–161.
39 L. V. Gulotta and S. A. Rodeo, *Clin. Sports Med.*, 2007, **26**, 509–524.
40 H. Gao, L. Wang, H. Jin, Z. Lin, Z. Li, Y. Kang, Y. Lyu, W. Dong, Y. Liu, D. Shi, J. Jiang and J. Zhao, *J. Funct. Biomater.*, 2022, **13**, 243.
41 Z. Yuan, D. Sheng, L. Jiang, M. Shafiq, A. U. R. Khan, R. Hashim, Y. Chen, B. Li, X. Xie, J. Chen, Y. Morsi, X. Mo and S. Chen, *Acta Biomater.*, 2022, **140**, 233–246.
42 A. C. Deymier, Y. An, J. J. Boyle, A. G. Schwartz, V. Birman, G. M. Genin, S. Thomopoulos and A. H. Barber, *Acta Biomater.*, 2017, **56**, 25–35.
43 D. Wang, X. Zhang, S. Huang, Y. Liu, B. S. Fu, K. K. Mak, A. M. Blocki, P. S. Yung, R. S. Tuan and D. F. E. Ker, *Biomaterials*, 2021, **272**, 120789.
44 C. Zhu, J. Qiu, S. Thomopoulos and Y. Xia, *Adv. Healthcare Mater.*, 2021, **10**, e2002269.
45 N. L. Millar, K. G. Silbernagel, K. Thorborg, P. D. Kirwan, L. M. Galatz, G. D. Abrams, G. A. C. Murrell, I. B. McInnes and S. A. Rodeo, *Nat Rev Dis Primers.*, 2021, **7**, 1.
46 L. M. Galatz, L. J. Sandell, S. Y. Rothermich, R. Das, A. Mastny, N. Havlioglu, M. J. Silva and S. Thomopoulos, *J. Orthop. Res.*, 2006, **24**, 541–550.
47 D. Kovacevic and S. A. Rodeo, *Clin. Orthop. Relat. Res.*, 2008, **466**, 622–633.
48 R. C. Locke, A. C. Abraham and M. L. Killian, *ACS Biomater. Sci. Eng.*, 2017, **3**, 2633–2643.
49 N. I. M. Fadilah, S. J. Phang, N. Kamaruzaman, A. Salleh, M. Zawani, A. Sanyal, M. Maarof and M. B. Fauzi, *Antioxidants*, 2023, **12**, 787.
50 D. E. Connor, J. A. Paulus, P. J. Dabestani, F. K. Thankam, M. F. Dilisio, R. M. Gross and D. K. Agrawal, *J. Bone Miner. Metab.*, 2019, **37**, 759–767.
51 H. H. Lu and S. Thomopoulos, *Annu. Rev. Biomed. Eng.*, 2013, **15**, 201–226.
52 H. M. Kim, L. M. Galatz, R. Das, N. Havlioglu, S. Y. Rothermich and S. Thomopoulos, *Connect. Tissue Res.*, 2011, **52**, 87–98.
53 S. Ruiz-Alonso, M. Lafuente-Merchan, J. Ciriza, L. Saenz-Del-Burgo and J. L. Pedraz, *J. Controlled Release*, 2021, **333**, 448–486.
54 A. Prabhath, V. N. Vernekar, E. Sanchez and C. T. Laurencin, *Int. J. Pharm.*, 2018, **544**, 358–371.
55 Y. Ishibashi, N. Adachi, H. Koga, E. Kondo, R. Kuroda, T. Mae and Y. Uchio, *J. Orthop. Sci.*, 2020, **25**, 6–45.
56 J. Goldman, *Arthroscopy*, 2012, **28**, 1049.
57 J. L. Carey and K. G. Shea, *J. Am. Acad. Orthop. Surg.*, 2015, **23**, e6–e8.
58 S. Weber and J. Chahal, *J. Am. Acad. Orthop. Surg.*, 2020, **28**, e193–e201.
59 M. S. Davey, E. T. Hurley, P. J. Carroll, J. G. Galbraith, F. Shannon, K. Kaar and H. Mullett, *Arthroscopy*, 2023, **39**, 452–458.
60 Y. Xu, W. X. Zhang, L. N. Wang, Y. Q. Ming, Y. L. Li and G. X. Ni, *World J. Stem Cells*, 2021, **13**, 753–775.
61 D. Figueroa, F. Figueroa, R. Calvo, A. Vaisman, X. Ahumada and S. Arellano, *Arthroscopy*, 2015, **31**, 981–988.
62 W. C. Lai, B. C. Iglesias, B. J. Mark and D. Wang, *Arthroscopy*, 2021, **37**, 2318–2333.e3.
63 M. Valencia Mora, M. A. Ruiz Iban, J. Diaz Heredia, R. Barco Laakso, R. Cuellar and M. Garcia Arranz, *World J. Stem Cells*, 2015, **7**, 691–699.
64 P. Hernigou, C. H. Flouzat Lachaniette, J. Delambre, S. Zilber, P. Duffiet, N. Chevallier and H. Rouard, *Int. Orthop.*, 2014, **38**, 1811–1818.
65 D. M. Dohan Ehrenfest, L. Rasmusson and T. Albrektsson, *Trends Biotechnol.*, 2009, **27**, 158–167.
66 A. L. L. de Andrade, A. V. Sardeli, T. A. Garcia, B. Livani and W. D. Belangero, *J. Sports Med. Phys. Fitness*, 2021, **49**, 2854–2858.
67 A. M. de Almeida, M. K. Demange, M. F. Sobrado, M. B. Rodrigues, A. Pedrinelli and A. J. Hernandez, *J. Sports Med. Phys. Fitness*, 2012, **40**, 1282–1288.
68 X. Dong, Q. Zhao, L. Xiao, Q. Lu and D. L. Kaplan, *Biomacromolecules*, 2016, **17**, 3000–3006.
69 D. H. Chow, P. K. Suen, L. H. Fu, W. H. Cheung, K. S. Leung, M. W. Wong and L. Qin, *J. Sports Med. Phys. Fitness*, 2012, **40**, 2862–2871.
70 S. R. Angle, K. Sena, D. R. Sumner and A. S. Virdi, *Ultrasonics*, 2011, **51**, 281–288.
71 Z. M. Ying, T. Lin and S. G. Yan, *J. Zhejiang Univ., Sci., B*, 2012, **13**, 955–963.
72 L. Wang, L. Qin, H. B. Lu, W. H. Cheung, H. Yang, W. N. Wong, K. M. Chan and K. S. Leung, *J. Sports Med. Phys. Fitness*, 2008, **36**, 340–347.
73 I. A. Trantos, E. S. Vasiliadis, F. S. Giannoulis, E. Pappa, F. Kakridonis and S. G. Pneumaticos, *J. Clin. Med.*, 2023, **12**, 581.
74 J. Cai, J. Wang, K. Ye, D. Li, C. Ai, D. Sheng, W. Jin, X. Liu, Y. Zhi, J. Jiang, J. Chen, X. Mo and S. Chen, *Int. J. Nanomed.*, 2018, **13**, 3481–3492.
75 J. Xu, Z. Ye, K. Han, T. Zheng, T. Zhang, S. Dong, J. Jiang, X. Yan, J. Cai and J. Zhao, *J. Sports Med. Phys. Fitness*, 2022, **50**, 662–673.
76 Y. Liu and C. Chen, *Adv. Drug Delivery Rev.*, 2016, **103**, 76–89.
77 S. Li, S. Xu, X. Liang, Y. Xue, J. Mei, Y. Ma, Y. Liu and Y. Liu, *Adv. Healthcare Mater.*, 2021, **10**, e2100078.
78 S. Kargozar, F. Baino, S. Hamzehlou, M. R. Hamblin and M. Mozafari, *Chem. Soc. Rev.*, 2020, **49**, 5008–5057.
79 Z. Abpeikar, M. Safaei, A. Akbar Alizadeh, A. Goodarzi and G. Hatam, *Int. J. Pharm.*, 2023, **633**, 122615.
80 E. Garbayo, S. Pascual-Gil, C. Rodriguez-Nogales, L. Saludas, A. Estella-Hermoso de Mendoza and M. J. Blanco-Prieto, *Wiley Interdiscip. Rev.: Nanomed. Nanobiotechnol.*, 2020, **12**, e1637.
81 J. Xie, X. Li, J. Lipner, C. N. Manning, A. G. Schwartz, S. Thomopoulos and Y. Xia, *Nanoscale*, 2010, **2**, 923–926.
82 J. Xue, T. Wu, Y. Dai and Y. Xia, *Chem. Rev.*, 2019, **119**, 5298–5415.

83 C. O. Chantre, G. M. Gonzalez, S. Ahn, L. Cera, P. H. Campbell, S. P. Hoerstrup and K. K. Parker, *ACS Appl. Mater. Interfaces*, 2019, **11**, 45498–45510.
84 E. E. Brown, M. Pierre and G. Laborie, *Biomacromolecules*, 2007, **8**, 3074–3081.
85 X. b Xing, Y. q Wang and B. j Li, *Opt. Express*, 2008, **16**(14), 10815–10822.
86 J. R. Porter, A. Henson and K. C. Popat, *Biomaterials*, 2009, **30**, 780–788.
87 P. Wang, H. Lv, X. Cao, Y. Liu and D. G. Yu, *Polym.*, 2023, **15**, 921.
88 G. C. Ingavle and J. K. Leach, *Tissue Eng., Part B*, 2014, **20**, 277–293.
89 M. Doostmohammadi, H. Forootanfar and S. Ramakrishna, *Mater. Sci. Eng., C*, 2020, **109**, 110521.
90 X. Zhao, Y. Zhou, J. Li, C. Zhang and J. Wang, *J. Biomed. Mater. Res., Part B*, 2022, **110**, 289–301.
91 J. Kang, J. Y. Hwang, M. Huh and S. I. Yun, *Macromol. Res.*, 2020, **28**, 835–843.
92 S. Zhang, *Nat. Biotechnol.*, 2003, **21**, 1171–1178.
93 C. P. Barnes, S. A. Sell, E. D. Boland, D. G. Simpson and G. L. Bowlin, *Adv. Drug Delivery Rev.*, 2007, **59**, 1413–1433.
94 Y. Zhao, M. Tanaka, T. Kinoshita, M. Higuchi and T. Tan, *J. Controlled Release*, 2010, **142**, 354–360.
95 N. Saveh-Shemshaki, S. N. Lakshmi and C. T. Laurencin, *Acta Biomater.*, 2019, **94**, 64–81.
96 C. Yu, T. Wang, H. Diao, N. Liu, Y. Zhang, H. Jiang, P. Zhao, Z. Shan, Z. Sun, T. Wu, X. Mo and T. Yu, *Adv. Fiber Mater.*, 2022, **4**, 908–922.
97 P. A. Agudelo-Garcia, J. K. De Jesus, S. P. Williams, M. O. Nowicki, E. A. Chiocca, S. Liyanarachchi, P. K. Li, J. J. Lannutti, J. K. Johnson, S. E. Lawler and M. S. Viapiano, *Neoplasia*, 2011, **13**, 831–840.
98 K. M. Kennedy, A. Bhaw-Luximon and D. Jhurry, *Acta Biomater.*, 2017, **50**, 41–55.
99 A. Seetharam, J. Abad, A. Baessler and B. L. Badman, *Orthop. J. Sports Med.*, 2022, **10**, 23259671221094848.
100 F. Han, P. Zhang, Y. Sun, C. Lin, P. Zhao and J. Chen, *Int. J. Nanomed.*, 2015, **10**, 7333–7343.
101 A. Romeo, J. Easley, D. Regan, E. Hackett, J. Johnson, J. Johnson, C. Puttlitz and K. McGilvray, *Journal of shoulder and elbow surgery*, 2022, **31**, 402–412.
102 K. L. Moffat, I. N. Wang, S. A. Rodeo and H. H. Lu, *Clin. Sports Med.*, 2009, **28**, 157–176.
103 M. Qasim, D. S. Chae and N. Y. Lee, *Int. J. Nanomed.*, 2019, **14**, 4333–4351.
104 Z. Zhang, J. Hu and P. X. Ma, *Adv. Drug Delivery Rev.*, 2012, **64**, 1129–1141.
105 B. Ma, J. Xie, J. Jiang, F. D. Shuler and D. E. Bartlett, *Nanomed.*, 2013, **8**, 1459–1481.
106 S. Wei, Y. Wang, Y. Sun, L. Gong, X. Dai, H. Meng, W. Xu, J. Ma, Q. Hu, X. Ma, J. Peng and X. Gu, *Int. J. Biol. Macromol.*, 2023, **235**, 123861.
107 F. Alshomer, C. Chaves and D. M. Kalaskar, *J. Mater.*, 2018, **2018**, 1–17.
108 S. Font Tellado, W. Bonani, E. R. Balmayor, P. Foehr, A. Motta, C. Migliaresi and M. van Griensven, *Tissue Eng., Part A*, 2017, **23**, 859–872.
109 S. Patel, J. M. Caldwell, S. B. Doty, W. N. Levine, S. Rodeo, L. J. Soslowsky, S. Thomopoulos and H. H. Lu, *J. Orthop. Res.*, 2018, **36**, 1069–1077.
110 J. Xie, B. Ma, P. L. Michael and F. D. Shuler, *Macromol. Biosci.*, 2012, **12**, 1336–1341.
111 N. Jiang, J. He, W. Zhang, D. Li and Y. Lv, *Mater. Sci. Eng., C*, 2020, **110**, 110711.
112 W. Liu, J. Lipner, J. Xie, C. N. Manning, S. Thomopoulos and Y. Xia, *ACS Appl. Mater. Interfaces*, 2014, **6**, 2842–2849.
113 Z. Lin, X. Zhao, S. Chen and C. Du, *J. Mater. Chem. B*, 2017, **5**, 1015–1027.
114 T. Wu, H. Li, J. Xue, X. Mo and Y. Xia, *Angew. Chem., Int. Ed.*, 2019, **58**, 16416–16421.
115 J. Lipner, W. Liu, Y. Liu, J. Boyle, G. M. Genin, Y. Xia and S. Thomopoulos, *J. Mech. Behav. Biomed. Mater.*, 2014, **40**, 59–68.
116 P. Chen, L. Li, L. Dong, S. Wang, Z. Huang, Y. Qian, C. Wang, W. Liu and L. Yang, *ACS Biomater. Sci. Eng.*, 2021, **7**, 841–851.
117 W. Su, Z. Wang, J. Jiang, X. Liu, J. Zhao and Z. Zhang, *Int. J. Nanomed.*, 2019, **14**, 1835–1847.
118 S. Zhao, X. Zhao, S. Dong, J. Yu, G. Pan, Y. Zhang, J. Zhao and W. Cui, *J. Mater. Chem. B*, 2015, **3**, 990–1000.
119 J. He, N. Jiang, T. Qin, W. Zhang, Z. Liu, Y. Liu and D. Li, *J. Mater. Chem. B*, 2017, **5**, 8579–8590.
120 M. Mittal, M. R. Siddiqui, K. Tran, S. P. Reddy and A. B. Malik, *Antioxid. Redox Signaling*, 2014, **20**, 1126–1167.
121 M. S. Hu, Z. N. Maan, J. C. Wu, R. C. Rennert, W. X. Hong, T. S. Lai, A. T. Cheung, G. G. Walmsley, M. T. Chung, A. McArdle, M. T. Longaker and H. P. Lorenz, *Ann. Biomed. Eng.*, 2014, **42**, 1494–1507.
122 K. T. Shalumon, C. Sheu, C. H. Chen, S. H. Chen, G. Jose, C. Y. Kuo and J. P. Chen, *Acta Biomater.*, 2018, **72**, 121–136.
123 Y. Liu, C. Li, Z. Feng, B. Han, D. G. Yu and K. Wang, *Biomolecules*, 2022, **12**, 1727.
124 C. J. Weng, Y. C. Wu, M. Y. Hsu, F. P. Chang and S. J. Liu, *Membr.*, 2022, **12**, 529.
125 J. Ye, M. Gong, J. Song, S. Chen, Q. Meng, R. Shi, L. Zhang and J. Xue, *Pharmaceutics*, 2022, **14**, 1273.
126 Q. Zhu, Z. Ma, H. Li, H. Wang and Y. He, *RSC Adv.*, 2019, **9**, 15582–15592.
127 X. Ni, X. Xing, Y. Deng and Z. Li, *Pharmaceutics*, 2023, **15**, 982.
128 C. Huang, S. J. Soenen, J. Rejman, B. Lucas, K. Braeckmans, J. Demeester and S. C. De Smedt, *Chem. Soc. Rev.*, 2011, **40**, 2417–2434.
129 M. A. Fernandez-Yague, A. Trotier, S. Demir, S. A. Abbah, A. Larranaga, A. Thirumaran, A. Stapleton, S. A. M. Tofail, M. Palma, M. Kilcoyne, A. Pandit and M. J. Biggs, *Adv. Mater.*, 2021, **33**, e2008788.
130 D. Denning, J. I. Kilpatrick, E. Fukada, N. Zhang, S. Habelitz, A. Fertala, M. D. Gilchrist, Y. Zhang, S. A. M. Tofail and B. J. Rodriguez, *ACS Biomater. Sci. Eng.*, 2017, **3**, 929–935.

131 D. Denning, M. T. Abu-Rub, D. I. Zeugolis, S. Habelitz, A. Pandit, A. Fertala and B. J. Rodriguez, *Acta Biomater.*, 2012, **8**, 3073–3079.
132 G. J. Fu, L. Y. Lu, Z. Y. Pan, A. Fan and F. Yin, *Regener. Med.*, 2021, **16**(4), 359–372.
133 M. L. Killian and S. Thomopoulos, *FASEB J.*, 2016, **30**, 301–311.
134 T. Gong, T. Liu, L. Zhang, W. Ye, X. Guo, L. Wang, L. Quan and C. Pan, *ACS Biomater. Sci. Eng.*, 2018, **4**, 240–247.
135 T. Yoshikawa, Y. Mifune, A. Inui, H. Nishimoto, K. Yamaura, S. Mukohara, I. Shinohara and R. Kuroda, *Antioxidants*, 2022, **11**, 743.
136 A. Liguori, S. Pandini, C. Rinoldi, N. Zaccheroni, F. Pierini, M. L. Focarete and C. Gualandi, *Macromol. Rapid Commun.*, 2022, **43**, e2100694.
137 M. Bao, X. Lou, Q. Zhou, W. Dong, H. Yuan and Y. Zhang, *ACS Appl. Mater. Interfaces*, 2014, **6**, 2611–2621.
138 T. Gong, W. Li, H. Chen, L. Wang, S. Shao and S. Zhou, *Acta Biomater.*, 2012, **8**, 1248–1259.
139 L. F. Tseng, P. T. Mather and J. H. Henderson, *Acta Biomater.*, 2013, **9**, 8790–8801.
140 K. A. Davis, K. A. Burke, P. T. Mather and J. H. Henderson, *Biomaterials*, 2011, **32**, 2285–2293.
141 M. Guo, G. Zhou, Z. Liu, J. Liu, J. Tang, Y. Xiao, W. Xu, Y. Liu and C. Chen, *Sci. Bull.*, 2018, **63**, 92–100.
142 K. Xu, S. Li, Y. Zhou, X. Gao, J. Mei and Y. Liu, *Pharmaceutics*, 2023, **15**, 1064.
143 Y. Gao and Q. Ma, *Smart Med.*, 2022, **1**, e2022001.
144 J. Zhang, J. Koh, J. Lu, S. Thiel, B. S. Leong, S. Sethi, C. Y. He, B. Ho and J. L. Ding, *PLoS Pathog.*, 2009, **5**, e1000282.
145 W. E. Teo and S. Ramakrishna, *Nanotechnology*, 2006, **17**, R89–R106.
146 S. U. D. Wani, S. P. Gautam, Z. L. Qadrie and H. V. Gangadharappa, *Int. J. Biol. Macromol.*, 2020, **163**, 2145–2161.
147 S. Qian, Z. Wang, Z. Zheng, J. Ran, J. Zhu and W. Chen, *Med. Sci. Monit.*, 2019, **25**, 269–278.
148 Y. Lin, L. Zhang, N. Q. Liu, Q. Yao, B. Van Handel, Y. Xu, C. Wang, D. Evseenko and L. Wang, *Int. J. Nanomed.*, 2019, **14**, 5831–5848.
149 S. K. Madhurakkat Perikamana, J. Lee, T. Ahmad, E. M. Kim, H. Byun, S. Lee and H. Shin, *Biomaterials*, 2018, **165**, 79–93.
150 Y. Lv, X. Sang, Z. Tian, S. Jiang, C. Li, Q. Guo, C. Wang, P. Hu and Y. Liu, *Int. J. Biol. Macromol.*, 2022, **217**, 180–187.
151 C. Liu, S. Jiang, W. Xu, X. Chen, R. He, K. Deng, H. Su, X. Yin, S. Su, T. Liang, L. Zhu, G. Hou, Y. Zhang, Y. Shi, W. Lv, L. Liu, Z. Guo, Y. Xu, T. Xu and K. Wang, *Int. J. Biol. Macromol.*, 2023, **245**, 125522.
152 K. Huang, W. Su, X. Zhang, C. A. Chen, S. Zhao, X. Yan, J. Jiang, T. Zhu and J. Zhao, *Chem. Eng. J.*, 2020, **392**, 123671.
153 M. Ramalingam, M. F. Young, V. Thomas, L. Sun, L. C. Chow, C. K. Tison, K. Chatterjee, W. C. Miles and C. G. Simon, Jr., *J. Biomater. Appl.*, 2013, **27**, 695–705.
154 K. Yu, T. Zhu, Y. Wu, X. Zhou, X. Yang, J. Wang, J. Fang, H. El-Hamshary, S. S. Al-Deyab and X. Mo, *Colloids Surf., B*, 2017, **151**, 314–323.
155 L. Yang, X. Li, Y. Wu, P. Du, L. Sun, Z. Yu, S. Song, J. Yin, X. Ma, C. Jing, J. Zhao, H. Chen, Y. Dong, Q. Zhang and L. Zhao, *Int. J. Nanomed.*, 2020, **15**, 8697–8715.
156 C. Wang, Z. Liu, N. Zhang, S. Huang, R. Mao, H. Wang, Q. Xia, C. C. Han, S. Xu and Y. Liu, *Mater. Des.*, 2021, **210**, 110019.
157 A. Romeo, J. Easley, D. Regan, E. Hackett, J. Johnson, J. Johnson, C. Puttlitz and K. McGilvray, *Journal of Shoulder and Elbow Surgery*, 2022, **31**, 402–412.
158 S. Samavedi, C. Olsen Horton, S. A. Guelcher, A. S. Goldstein and A. R. Whittington, *Acta Biomater.*, 2011, **7**, 4131–4138.
159 K. Chen, Y. Li, Y. Li, W. Pan and G. Tan, *Macromol. Biosci.*, 2023, **23**, e2200380.
160 L. Li, Y. Zuo, Q. Zou, B. Yang, L. Lin, J. Li and Y. Li, *ACS Appl. Mater. Interfaces*, 2015, **7**, 22618–22629.
161 A. Bharadwaz and A. C. Jayasuriya, *Mater. Sci. Eng., C*, 2020, **110**, 110698.
162 J. Sun, L. Li, F. Xing, Y. Yang, M. Gong, G. Liu, S. Wu, R. Luo, X. Duan, M. Liu, M. Zou and Z. Xiang, *Stem Cell Res. Ther.*, 2021, **12**, 591.
163 A. Raslan, L. Saenz Del Burgo, J. Ciriza and J. L. Pedraz, *Int. J. Pharm.*, 2020, **580**, 119226.
164 Y.-C. Chou, W.-L. Yeh, C.-L. Chao, Y.-H. Hsu, Y.-H. Yu, J.-K. Chen and S.-J. Liu, *Int. J. Nanomed.*, 2016, **11**, 4173–4186.
165 P. Zhang, F. Han, T. Chen, Z. Wu and S. Chen, *Biomater. Sci.*, 2020, **8**, 871–883.
166 F. Han, P. Zhang, T. Chen, C. Lin, X. Wen and P. Zhao, *Int. J. Nanomed.*, 2019, **14**, 9159–9172.
167 H. Li, T. Wu, J. Xue, Q. Ke and Y. Xia, *Macromol. Rapid Commun.*, 2020, **41**, e1900579.
168 K. L. Moffat, A. S. P. Kwei, J. P. Spalazzi, S. B. Doty, W. N. Levine and H. H. Lu, *Tissue Eng., Part A*, 2009, **15**(1), 115–126.
169 W. Liu, Y.-C. Yeh, J. Lipner, J. Xie, H.-W. Sung, S. Thomopoulos and Y. Xia, *Langmuir*, 2011, **27**, 9088–9093.

